A review of carbon nanotubes in modern electrochemical energy storage

SONG Yao-ming[1,2], QIU Shi-xin[1,2], FENG Shu-xin[1,2], ZUO Rui[1], ZHANG Ya-ting[1], JIA Ke[1], XIA Xue[1,2], CHEN Ming-ming[1,*], JI Ke-meng[1,2,*], WANG Cheng-yang[1]

（1. *Key Laboratory for Green Chemical Technology of Ministry of Education*, *School of Chemical Engineering and Technology*, *Tianjin University*, *Tianjin* 300350, *China*;
2. *National Industry-Education Platform for Energy Storage*, *Tianjin University*, *Tianjin* 300350, *China*）

Abstract: The quest for sustainable energy storage solutions is more critical than ever, with the rise in global energy demand and the urgency of transition from fossil fuels to renewable sources. Carbon nanotubes (CNTs), with their exceptional electrical conductivity and structural integrity, are at the forefront of this endeavor, offering promising ways for the advance of electrochemical energy storage (EES) devices. This review provides an analysis of the synthesis, properties, and applications of CNTs in the context of EES. We explore the evolution of CNT synthesis methods, including arc discharge, laser ablation, and chemical vapor deposition, and highlight the recent developments in metal-organic framework-derived CNTs and a novel CNT aggregate with a three-dimensional ordered macroporous structure. We also examine the role of CNTs in improving the performance of various EES devices such as lithium-ion, lithium-metal, lithium-sulfur, sodium, and flexible batteries as well as supercapacitors. We underscore the challenges that remain, including the scalability of CNT synthesis and the integration of CNTs in electrode materials, and propose potential solutions and future research directions. The review presents a forward-looking perspective on the pivotal role of CNTs in shaping the future of sustainable EES technologies.

Key words: Carbon nanotubes; CNT synthesis; Metal-ion batteries; Lithium-sulfur batteries; Flexible batteries; Supercapacitors

1 Introduction

1.1 Background

The extensive use of traditional chemical energy sources, such as coal, petroleum, and natural gas, has significantly contributed to industrialization and urbanization. However, this overuse has also led to numerous serious issues. Non-renewable resources face the risk of depletion, and there is a concomitant rise in environmental pollution, including the annual increase in global CO_2 emissions and the melting of glaciers[1]. Consequently, the development of green, efficient, and safe new renewable energy technologies is quite urgent. Electrochemical energy storage (EES) technology has garnered extensive interest from researchers due to its convenience, high efficiency, and environmental friendliness[2].

Since their commercialization in the 1990s, lithium-ion batteries (LIBs) have been favored for their excellent cycle stability and mature technology, leading to widespread use in electronic products[3]. However, the escalating global demand for sustainable energy solutions, driven by the burgeoning sectors of mobile electronics and electric vehicles, has intensified the quest for more efficient and economical energy storage technologies[4]. Despite their prevalence, LIBs have limitations in energy density and resource availability, necessitating the exploration of alternative EES systems[5].

Lithium metal batteries (LMBs) are regarded as one of the most promising EES technologies of the future due to their lowest electrochemical potential of –3.04 V (compared to standard hydrogen electrodes, SHE) and an ultra-high theoretical specific capacity of 3 860 mAh g^{-1}[6]. Despite these advantages, the high reactivity of lithium metal (Li) can lead to side reactions with the electrolyte, resulting in the formation of

Received date: 2024-05-16; **Revised date:** 2024-07-22
Corresponding author: CHEN Ming-ming, Professor. E-mail: chmm@tju.edu.cn;
JI Ke-meng, Associate Professor. E-mail: kmji@tju.edu.cn
Author introduction: SONG Yao-ming, Master student. E-mail: ymsong127@tju.edu.cn

an unstable solid electrolyte interfacial (SEI) film. This instability leads to non-uniform current density during Li deposition and causes the growth of Li dendrites, which seriously destabilizes battery operation and present significant safety hazards[6]. Among various LMBs, lithium-sulfur batteries (LSBs) stand out as a particularly typical example. Capitalizing on the Earth's abundant sulfur (S) content, LSBs offer a high theoretical specific capacity of 1 675 mAh g^{-1} and have thus become a popular research focus[7]. However, the insulating nature of sulfur and the shuttling effect of lithium polysulfides (LiPSs) during charging and discharging in ether-based electrolytes result in the loss of active material, severely limiting the cycling stability and rate capability of LSBs[8]. Sodium-ion batteries (SIBs) and sodium-metal batteries (SMBs) which utilize the much more abundant element sodium (Na) in the Earth's crust, offer a potential advantage in material availability over Li-based energy storage systems. Nevertheless, similar to LIBs and LMBs, these Na-based batteries still confront comparable safety challenges[9].

In contrast, supercapacitors excel in power density but typically lag in energy density compared to batteries. They store charge through electric double-layer capacitors (EDLCs) and pseudocapacitors, with the latter gaining attention for their higher specific capacitance due to surface Faraday reactions[10]. The efficient transfer of ions and electrons at the microscopic level within EES devices is crucial, and conductive agents play a pivotal role in this charge-storage process[11].

Carbon nanotechnology, with its environmentally friendly approach, presents innovative solutions by offering materials that boast enhanced efficiency and unique properties[12]. Among the spectrum of carbon nanomaterials, including graphene, carbon nanofibers (CNFs), carbon nanosheets, and hybrid bulk carbon, carbon nanotubes (CNTs) stand out. They exhibit exceptional electronic conductivity, robust mechanical strength, excellent chemical stability, high aspect ratio, and large specific surface area[13–15]. These characteristics endow CNTs with significant potential for EES applications, where they can be utilized effectively both as active materials and as conductive additives. Since the discovery of CNTs, a multitude of studies has been conducted worldwide, spanning fields including media, transportation, energy, health, and the environment[16]. This review complements previous works[16] by providing updated statistics on publications and patents from 2000 to 2023, as illustrated in Fig. 1a, focusing on articles and patents related to CNTs and EES. The consistent annual increase in the number of patents and publications related to CNTs indicates the sustained and growing interest in CNTs-related research within the scientific community.

1.2 Introduction to CNTs

1.2.1 Classification of CNTs

CNTs are tubular nanostructures that have been a focal point of research and industrial interest due to their unique properties and potential applications in

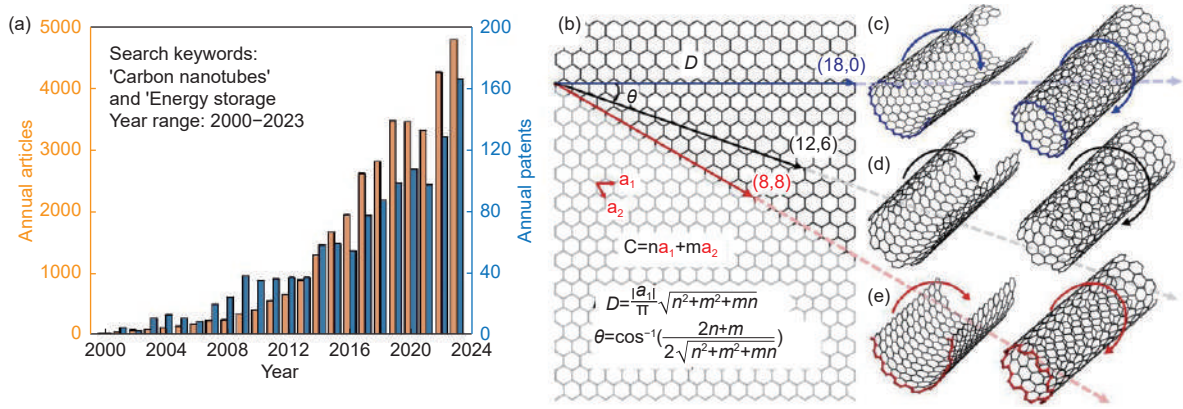

Fig. 1 (a) Statistics of articles and patents related to CNTs from 2000 to 2023. (b–e) Schematic diagram of chirality index of CNTs[16]. (Reproduced with permission)

various fields. The initial terminology for CNTs was inconsistent, with terms such as “carbon filaments” or “carbon nanofibers” being used. The concept dates back to 1890, stemming from observations in the chemical industry where they were produced by the decomposition of hydrocarbons over small-molecule metal catalyst particles, such as iron or cobalt-nickel[17]. The electron microscope’s invention later allowed for more accurate characterization of CNTs’ intricate structure, leading to the discovery by S. Iijima in 1991, who identified a new carbon isotope and detailed the helical arrangement of carbon atoms in CNTs[18].

CNTs are characterized by a helical vector (Chiral Vector) derived from the hexagonal lattice’s basis vectors (a_1, a_2), expressed as $C = na_1 + ma_2$ (Fig. 1b–e). The indices (n, m) define the chirality, which is the CNT’s curl direction[19]. Based on the chiral index, single-walled carbon nanotubes (SWCNTs) are classified into 3 types: Zigzag ($m = 0$), Armchair ($n = m$), and Chiral (other values), which affects the electronic properties[20]. Theoretical analysis indicates that SWCNTs with $(n - m) = 3i$ (i being an integer) exhibit metallic properties (the density of states at the Fermi level is not zero), while other values result in semiconducting properties (the density of states at the Fermi level is zero)[21]. This distinction forms the basis for the second classification of CNTs.

CNTs can also be categorized based on the number of graphite layers into SWCNTs and multi-walled carbon nanotubes (MWCNTs). MWCNTs, which consist of multiple layers of graphene, may exhibit varying chirality across their layers, complicating their electron transport properties. However, most MWCNTs display metallic properties and excellent conductivity[22].

1.2.2　Properties of CNTs

CNTs are ideal one-dimensional (1D) materials, characterized by their exceptional aspect ratio, which endows them with superior mechanical, electrical, and thermal properties[23]. The sp^2 hybridization of CNTs’ carbon atoms eliminates dangling bonds, ensuring chemical stability, and forms σ-bonds that are among the strongest known. Theoretical calculations[24] suggest CNTs can achieve elastic modulus of 5 TPa, approximately 25 times stronger than steel. The chemical bond between C—C makes the tensile strength of CNT go up to 100 GPa[25], 50 times that of steel, and the elongation at break is as high as 15%–20%. Besides, the Young’s modulus of the defect-free CNT is as high as 1 TPa or more[26], 5 times that of steel, which are much higher than any other materials currently available. However, synthesis defects can reduce actual strength. The exceptional mechanical properties of CNTs, characterized by their strength and flexibility, make them ideal candidates for the construction of self-supporting and flexible electrodes in EES systems[27,28]. These properties are crucial for the development of durable and adaptable energy storage devices that can withstand real-world conditions. Post-treatments of SWCNTs, such as oxidation or water-assisted synthesis, can improve their purity and reduce their structural defects, thereby enhancing the mechanical properties. Pre-treatments and post-treatments of MWCNTs, such as high-temperature annealing, or chemical functionalization, can dramatically change the microstructures and surface states, which can in turn affect the mechanical properties. For example, high-temperature annealing improves the ordered structure and reduces the defects of MWCNTs, while chemical functionalization improves the compatibility with solvents and purity[23].

Electrically, CNTs exhibit unique band structures that facilitate excellent electron transport. Semiconductor-type CNTs are ideal for microelectronic devices due to their gate-controllable properties[29]. Metal-type CNTs exhibit long free-carrier paths, enabling ballistic transport where electrons face minimal resistance within the material[30]. Ballistic transport has been observed in both SWCNTs and MWCNTs, promising for supercapacitor applications due to their high current density tolerance (10^9 A cm^{-2})[31]. Chlorine doping of MWCNTs enhances their conductivity by modifying the helicity and morphology, which in turn influences their electrical properties. CNTs possess exceptional electrical conductivity due to their

large aspect ratio and unique outer surface area. These characteristics make them excellent materials for use in supercapacitors and battery electrodes, where efficient charge transfer and storage are paramount. Moreover, CNTs demonstrate electronic conductivity that is 3 to 20 000 times greater than that of conventional carbon black conductors (Table 1), underscoring their suitability for EES applications[32–35].

Thermally, CNTs exhibit excellent thermal conductivity, similar to other carbon allotropes like diamond and graphite[36]. Ordered CNT arrangements can achieve thermal conductivities exceeding 200 W m^{-1} K^{-1}, a feature that, combined with their low density[37], makes them highly desirable for thermal interface materials. This property is particularly advantageous for applications where weight is a critical factor, such as in aerospace or portable electronics. SWCNTs, in particular, have a higher thermal conductivity per unit mass than MWCNTs. This superiority stems from the higher phonon mean free path in SWCNTs, which facilitates more efficient phonon transport along the tube. The efficient heat dissipation capabilities of CNTs are crucial for extending the operational life of batteries and supercapacitors. By preventing thermal buildup—a common issue that degrades the performance and safety[38,39]—CNTs can help maintain the stability and longevity of these energy storage devices.

CNTs also exhibit enhanced field emission characteristics due to their high aspect ratio and nanometer-sized curvatures, allowing electron emission at lower voltages. Their stable chemical properties, mechanical strength, and high melting points make them competitive in field emission applications[40].

Furthermore, CNTs possess an ultrablack property due to their unique micro-nanostructures, which can enhance the absorption of infrared radiation, approaching the performance of a blackbody. Vanta Black, developed by Surrey NanoSystems (UK), is an example of CNT-based material with an emissivity of 0.998 in the visible and infrared spectrum, making it the darkest man-made substance[41].

1.2.3 Different roles of CNTs

SWCNTs and MWCNTs each possess unique attributes that influence their applications and roles. SWCNTs are primarily utilized in nanoelectronic devices[42], EES[43], composite reinforcement[44], and as catalysts[45]. In contrast, MWCNTs have a diverse range of applications, including EES[46], hydrogen storage[47], electromagnetic shielding[48], and biomedicine[49]. It is evident that both SWCNTs and MWCNTs are extensively used in EES applications, albeit they display significant differences. SWCNTs, known for their exceptional electrical conductivity and mechanical strength as mentioned above, excel in supercapacitors and LIBs, particularly in the development of flexible batteries. These properties can enhance the EES capacity and cycle life of EES devices[50]. MWCNTs are frequently employed as conductive agents in EES devices, effectively improving the rate performance of batteries. Moreover, their electrochemical properties can be enhanced through surface modification, making them suitable for use as electrode materials in supercapacitors[51]. Besides, the application of SWCNTs in EES devices can be somewhat limited due to their large bundle size and dispersion challenges. Nonetheless, their dispersion can be improved through treatment with strong acids and the use of dispersion aids, which can broaden their application in EES devices[52]. MWCNTs, being relatively

Table 1 Comparison of properties of different carbon materials[34,35]

Carbon	Properties			
	Specific gravity/(g cm^{-3})	Electrical conductivity/(S m^{-1})	Thermal conductivity/(W m^{-1} K^{-1})	Surface area/(m^2 g^{-1})
Carbon black	0.1–2.0	0.05−0.30	0.4	10–1443
CNTs	0.8–1.8	$1–10^4$	2000–6000	50–1315
CNFs	1.5–2.0	10^{-9}−10	5–1600	20–2500
Graphite	1.9–2.3	40^p 0.03^c	298^p 2.2^c	1−20
Graphene	2.3	10^4	600–5000	500–2630

Note: *p*: in-plane; *c*: *c*-axis

well dispersed, can be applied in energy storage devices using simple physical dispersion methods.

We further emphasize the distinction between the applications of metallic and semiconducting CNTs. The majority of MWCNTs exhibit metallic properties and possess excellent electrical conductivity, making them ideal for crafting conductive electrodes for both supercapacitors and batteries. In contrast, SWCNTs, due to their unique chiral characteristics, can possess either metallic or semiconducting properties. Metallic SWCNTs are particularly notable for their resistance, which does not increase with length, facilitating ballistic transport. This property is beneficial in avoiding the drawback of severe heat dissipation at high current densities[53]. The ability of metallic SWCNTs to conduct electricity without an increase in resistance over length makes them advantageous for applications requiring high current densities, minimizing the risk of thermal issues that can degrade performance and safety in EES devices. Moreover, metallic SWCNTs exhibit significantly higher electrical conductivity than graphite, up to 10^6 S m^{-1}, due to stronger π-electron off-domain interactions, which is advantageous in EES applications[53]. Semiconducting SWCNTs, characterized by their inelastic scattering-based carrier transport, demonstrate higher electron mobility than intrinsic silicon-based semiconducting materials, reaching 10^5 cm^2 V^{-1} s^{-1}, which is approximately 10 times that of silicon[54]. Their band gap is also adjustable by modifying the tube diameter of CNT, making semiconducting SWCNTs primarily suitable for applications in field-effect transistors.

2 Preparation methods of CNTs

Currently, the prevalent methods for preparing CNTs include arc discharge (AD), laser ablation (LA), and chemical vapor deposition (CVD)[13]. Additionally, plasma-enhanced CVD (PECVD)[13] and alcohol-catalyzed CVD (ACVD) are also recognized techniques for CNT synthesis.

In recent years, innovative preparation methods have emerged, such as metal-organic framework (MOF)-based CNTs derived from MOFs[55]. Another innovation method involves the synthesis of CNTs at lower temperatures compared to traditional high-temperature methods[56]. However, these methods still have inherent limitations, including high costs, complex processes, harsh conditions, low product purity, and poor homogeneity. Our group has developed a novel CVD method for CNT preparation, resulting in a three-dimensional ordered macroporous (3DOM) structure with excellent electronic conductivity and a highly organized honeycomb architecture[57]. This structure significantly enhances ion and electron transmission, improves the material's electrical conductivity, and accelerates the electrochemical reactions in EES systems, demonstrating excellent performance and promising application prospects.

The CVD method is the most commonly used industrial technique for CNT production[58], with AD and LA methods also in use. While laboratory-scale preparation often yields more homogeneous results, industrial application of these methods can reveal various issues, such as poor material homogeneity, low purity, and the difficulty of achieving chiral control. High costs, particularly associated with AD and LA methods, significantly limit the rapid development of CNTs[58]. Based on our research findings[57], it is promising to envision the mass production of CNT materials with low cost, safety, reliability, homogeneity, and good conductivity in the near future. Consequently, the most important CNT preparation methods and their principles will be introduced in the subsequent sections.

2.1 Plasma synthesis methods

2.1.1 Arc discharge method

Among the various preparation techniques, the AD method stands out for its ability to produce high-quality CNTs. The fundamental principle involves passing a direct current between two graphite electrodes in an inert atmosphere, leading to the vaporization of the anode graphite rods and the subsequent formation and deposition of CNTs on the cathode's surface and the reaction chamber's walls, as depicted in Fig. 2a[59]. MWCNTs can be directly synthesized

without the need for metal catalysts, whereas the addition of metal catalysts such as Fe, Co and Ni to the anode facilitates the production of SWCNTs[60]. The introduction of metal particle catalysts into hydrocarbons also leads to the formation of CNTs, as these catalysts aid in the decomposition of gas molecules into carbon, which then forms CNTs along the metal tip[61]. However, it is important to note that the use of various metal catalysts can compromise the purity of the synthesized CNTs, making subsequent purification steps necessary.

CNTs synthesized via the AD method are known for their structural precision. However, the final structure and size of the CNTs are influenced by several factors, including the temperature within the reaction chamber, the concentration and type of catalyst used, and the presence of hydrogen[62]. A research led by Arora et al. has shown that the crystallinity of the material improves with an increase in the discharge current[63]. More recently, Madni et al. have made significant strides in developing a cost-effective synthesis and purification process for MWCNTs using the AD method[64]. A summary of CNT properties under various operating conditions is presented in Table 2[65–72].

2.1.2 Laser ablation method

The LA method, initially discovered by Smalley, is a technique used for the synthesis of CNTs[73]. It operates at temperatures ranging from 800 to 1 200 °C under a pressure of 500 Torr (1 Torr = 0.133 32 kPa) in an inert gas environment. A high-energy laser beam is directed at the graphitic material, causing it to evaporate and generate gaseous carbon. This gaseous carbon is subsequently catalyzed by a transition metal catalyst to form SWCNTs, as illustrated in Fig. 2b[59]. The LA method's core principle involves focusing a high-energy laser on graphite positioned within a quartz boat in the reaction chamber, leading to the evaporation of graphite and the production of CNTs. The characteristics of the laser, including its laser intensity, wavelength[74], and the local conditions near the evaporation zone[75], significantly influence the structure and properties of the synthesized CNTs. Additionally, factors such as the buffer gas pressure, chamber pressure, chemical composition, and ambi-

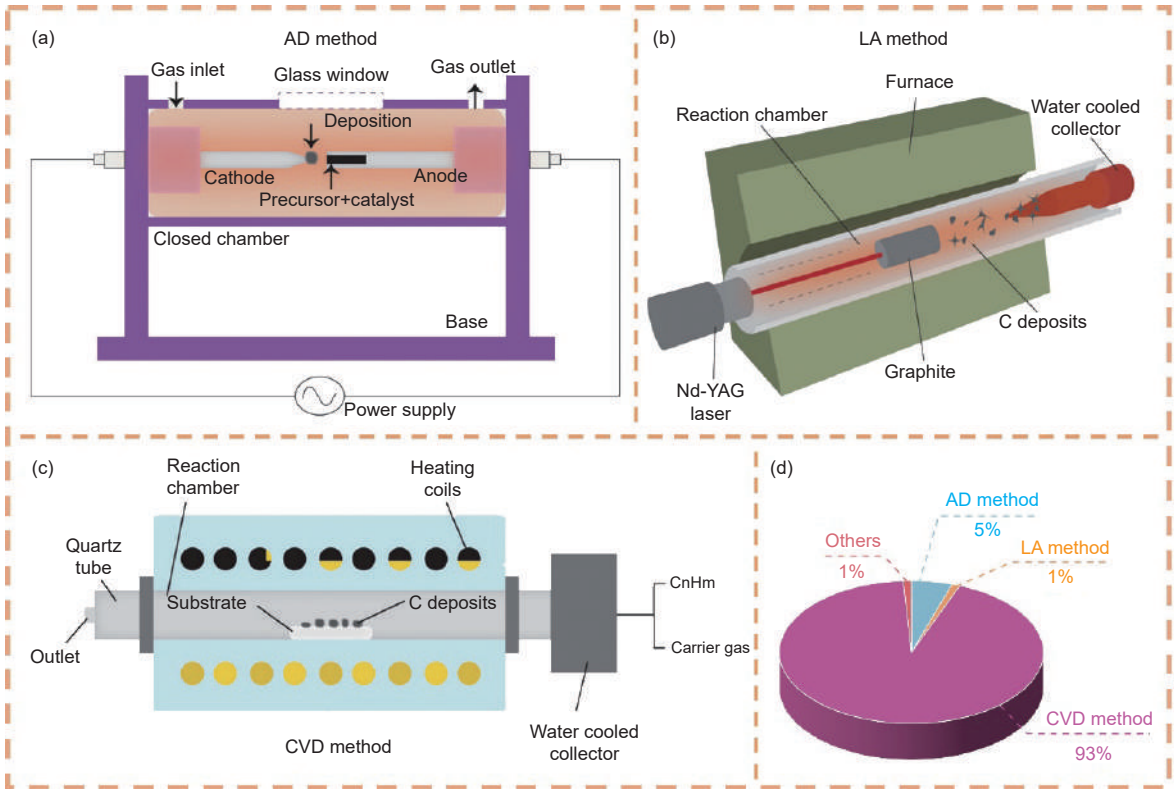

Fig. 2 (a–c) Schematic diagram of the main synthesis methods of CNTs[59]: (a) AD method (b) LA method, and (c) CVD method. (d) Distribution of different preparation methods. (Reproduced with permission)

Table 2　CNT properties via arc discharge method

CNT type	Diameter/nm	Inert gas	Pressure/Torr	Observation parameter		References
				Voltage/V	Current/A	
SWCNT	1.3−1.5	He	375	23−25	55	[65]
SWCNT	1.1–1.7	Ar	75	50	100	[66]
SWCNTs	1.3−2.7	H_2	240	−	120	[67]
MWCNTs	30–80	Ar	600–750	20	70	[68]
MWCNTs	20–60	Ar	760	380	6–20	[69]
MWCNTs	15−150	Ar	−	20−30	50−200	[70]
MWCNTs	−	−	−	−	90	[71]
MWCNTs	10−20	Air	0.0075	12	70	[72]

ent temperature greatly affect the final product's properties. Studies related to CNTs prepared by the LA method are detailed in Table 3[74,76–79].

The LA method's effectiveness in producing CNTs is significantly impacted by the catalyst selection and reaction temperature. Higher temperatures generally increase both the yield and diameter of the CNTs, but there is a threshold beyond which the catalyst's activity decreases, negatively affecting CNT growth. While the LA method is more conducive to SWCNT growth compared to the AD method, its industrial applications are limited due to the high cost of equipment and the complexity of the operation process.

2.2　Thermal synthesis method

Thermal synthesis methods, such as CVD, PECVD, floating catalyst chemical vapor deposition (FCCVD) and ACVD, are recognized for their energy efficiency, with synthesis temperatures generally below 1 200 °C[80]. These methods offer a lower cost and more controlled approach to CNT synthesis compared to plasma-based methods.

2.2.1　Chemical vapor deposition

CVD is a process where carbon atoms are deposited, and CNTs are formed through the catalytic decomposition of carbon monoxide or hydrocarbon gases (in liquid or solid form) at temperatures ranging from 500 to 1 200 °C[80]. The carbon source is first introduced into the reaction chamber, where, in the presence of a catalyst, it decomposes to form CNTs (Fig. 2c)[59]. Theoretically, any carbon-containing substance can serve as a carbon source for CNTs[81]. The CVD method offers advantages such as requiring a small amount of catalyst and allowing for precise control over CNT structure. It is commonly used in horizontal reactors that maintain a uniform temperature. The utilization rate distribution of different methods is shown in Fig. 2d.

The synthesis of CNTs by CVD method is influenced by several process parameters, including the type of carbon source, catalyst, reaction temperature, reaction time and gas flow rate[82]. The carbon source's structural orientation significantly affects the CNT properties. Linear hydrocarbon molecules, such as methane and acetylene, typically yield straight and hollow CNTs, while cyclic hydrocarbons like benzene and cyclohexane result in more curved structures[80]. The calcination temperature is crucial for synthesizing CNTs with varying properties. Yan et al. found that increasing the temperature increased the growth rate, density, and length of CNTs[83]. The gas flow rate also significantly influences the CNT production, with increased flow rates shortening the contact time between the carbon precursor and the cata-

Table 3　CNT properties via laser ablation methods using Ar as inert gas

CNT type	Diameter/nm	Length/μm	Pressure/Torr	Laser source	Temperature/°C	Catalyst	References
SWCNT	1.1–1.4	10–20	500	Pulsed Nd: YAG	800–1150	Co/Ni	[74]
SWCNTs	1.1−1.4	−	400	Nd: YAG	925	Co-Ni	[76]
SWCNT	10.0	−	0.75	Pulsed Nd: YAG	Ambient	Co-Fe	[77]
MWCNT	5.0−20.0	1−10	−	CO_2 laser	660	Fe	[78]
MWCNT	−	−	0.08	Solid state-focused: 10−80 mW	700−900	Fe	[79]

lyst, leading to fluctuations in CNT yield and grain size. The type of catalyst is another critical parameter. Huynh et al. synthesized CNTs using methane and Fe-rich and Cr-rich particles on a stainless steel foil as a catalyst[84]. The pretreatment of the steel foil is essential for CNT formation, with the size of the Fe and Cr particles closely related to the diameters of the synthesized CNTs. Transition metal atoms, such as Fe, Co, and Ni, generally exhibit better catalytic activity for CNT growth[13]. Table 4 summarizes the CNTs synthesized by the CVD methods[85–93].

The growth mechanism of CNTs has been a topic of debate. Baker and colleagues proposed key steps for CNT growth on the catalyst surface, observing single CNT growth under electron microscopy (Fig. 3a)[17,94]. Initially, hydrocarbons adsorb and decompose on the catalyst surface, with the generated carbon partially diffusing into the gas phase and partially dissolving into the catalyst. The dissolved carbon then diffuses within the catalyst before being deposited and growing on the particle's backside. However, it has also been shown that the activation energy of carbon diffusion through the catalyst surface is significantly lower than that of bulk diffusion[95]. More specifically, growth mode is also related to the type of catalyst. Kumar et al. described two growth modes: the tip-growth model and the base-growth model (Fig. 3b, c)[80]. In the tip-growth model, where the catalyst-substrate interaction is weak, hydrocarbons decompose at the metal's top, and carbon diffuses through the metal, with CNTs growing longer as long as the metal's top remains exposed to fresh hydrocarbon decomposition. The base-growth model occurs when the catalyst-substrate interaction is strong, and the metal has an obtuse contact angle with the substrate, leading to the formation of a hemispherical dome of carbon that extends upward, with the catalyst particles rooted in the substrate.

Research has shown that CNT growth is not strictly parallel to the graphite layer and may involve more complex processes. Helical, bidirectional, and branching CNTs have been observed (Fig. 3d–g)[17,96]. High-resolution transmission electron microscopy (HRTEM) has also shown that the graphite layer can grow along the catalyst's side, forming non-parallel "herringbone" or "cup-shaped" CNTs (Fig. 3h, i)[97]. In addition, CNT arrays with fewer defects have also received widespread attention, including ultralong (Fig. 3j)[98] or ultrapure (Fig. 3k)[99] CNT horizontal arrays and vertical arrays (Fig. 3l)[100].

2.2.2 Plasma enhanced chemical vapor deposition

PECVD is an innovative technique utilized for the synthesis of thin film materials through the chemical reaction of gaseous precursors in the presence of a glow discharge plasma[101]. This method is characterized by its low deposition temperature and minimal impact on the substrate's structure and physical properties[102], ensuring uniformity in the film's thickness and composition. The primary methods for sustaining glow discharges include radio frequency excitation, direct current (DC) high voltage excitation, pulsed excitation, and microwave excitation. Sato et al. have successfully synthesized CNTs using radio frequency plasma enhanced vapor deposition (RF-PECVD)[103], a process that involves the activation of a metal catalyst

Table 4 CNT properties by chemical vapor deposition method

CNT type	Diameter/nm	Length/μm	Inert gas	Temperature/°C	Time/min	Carbon source	Catalyst	References
SWCNT	1–3	–	Ar-He/H_2	550–750	10	Ethylene	Fe, Fe/Al, Co/Al_2O_3	[85]
SWCNT	0.8–1.3	10	H_2-N_2	850–950	30	Coal gas	Ferrocene	[86]
MWCNTs	31–36	–	Ar	850	60	Acetylene	Ferrocene	[87]
MWCNTs	10–21	–	H_2	1000	10–120	Methane	$MgMoO_4$	[88]
MWCNTs	10–140	–	H_2	800	5	Cyclohexane	Co, Fe, Al	[89]
MWCNTs	–	–	N_2	750	–	Xylene & Cyclohexanol	Ferrocene	[90]
MWCNT	106	8	NH_3	650−800	10	Acetylene	Stainless steel	[91]
MWCNT	10−50	–	Ar	400−1000	30	Ethanol	Stainless steel	[92]
MWCNTs	34	–	Ar	750	5–240	Benzene	Ferrocene	[93]

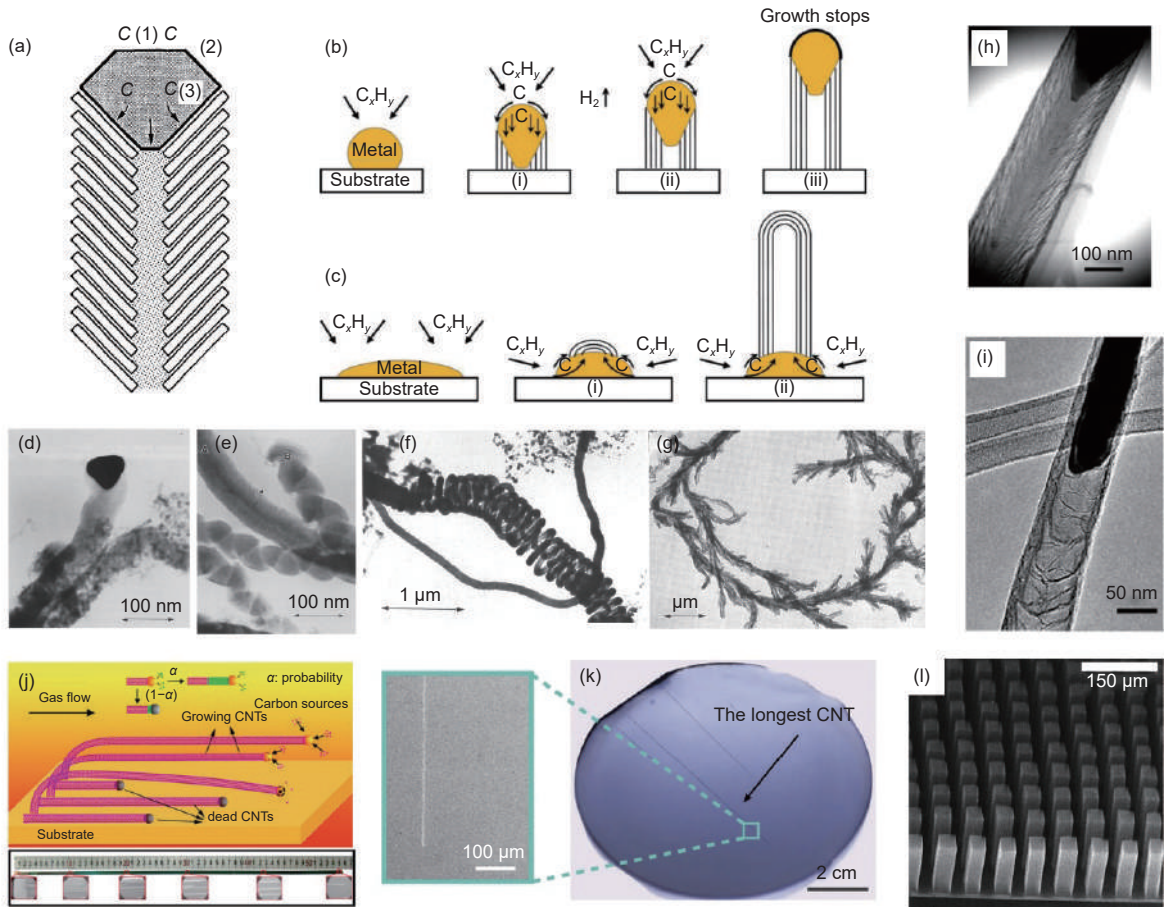

Fig. 3　(a) Schematic of the key steps involved in the growth of carbon nanofibers (CNFs): adsorption, diffusion and precipitation[17,94]. (b–c) Growth mechanisms of CNTs prepared by CVD method[80]: (b) tip-growth model and (c) base-growth model. (d–g) Different types of CNFs[17,96]: (d) whisker-like, (e–f) spiral and (g) branched. (h, i) Herringbone CNF[97]. (j) Horizontal array of ultralong CNTs (550 mm)[98]. (k) Ultrapure semiconducting CNT arrays[99]. (l) Vertical array of CNTs[100]. (Reproduced with permission)

on the substrate. This activation leads to the formation of nanoscale catalyst particles, which is crucial for the growth of CNTs. The formation of metal nanoparticles in the RF-PECVD process is highly sensitive and significantly influences the quality of CNT growth[102].

Compared to AD and LA methods, CVD offers a simpler and more cost-effective approach for synthesizing CNTs at low temperatures and atmospheric pressure. While the crystallinity of CNTs produced by arc and laser methods may surpass that of CVD-grown CNTs, the latter excels in terms of yield and purity[80]. Furthermore, CVD provides unparalleled control over the architecture of CNTs. Therefore, CVD is the most widely used technology (Fig. 2d).

The versatility of CVD is particularly highlighted by its compatibility with a broad spectrum of hydrocarbons, which can be in solid, liquid, or gaseous states, serving as carbon sources[104]. This flexibility significantly broadens the range of substrate materials that can be utilized for CNT synthesis. Furthermore, CVD facilitates the growth of CNTs in a couple of forms, including powders, thin or thick films, and in structures that can be aligned, tangled, straight, or coiled. The reaction parameters in CVD are notably malleable[105], which, in contrast to the more equipment-intensive and financially demanding AD and LA methods, makes CVD a more accessible and market-friendly technique. Essentially, CVD has been extensively adopted for the large-scale fabrication of CNTs, and there exists considerable potential for the future advancement of cost-effective and structurally precise CNT synthesis technologies.

2.3　Other synthesis methods of CNTs

Metal-organic framework (MOF) materials, known for their ordered porous crystalline structures

composed of metal ions or ion clusters linked by organic ligands, have emerged as a novel platform for the synthesis of CNTs. In 2013, Yang et al. pioneered the use of iron-doped zeolite imidazole framework (ZIF)-8 to produce nitrogen-doped CNT composites (NCNT) through pyrolysis under nitrogen, yielding a mixture of Zn-Fe-ZIF crystals and dicyandiamide[106]. This method has attracted attention for its potential to enhance the electrochemical performance and catalytic properties of CNT composites[107]. In particular, researchers have explored the in-situ transformation of MOFs into CNT-based composites, employing techniques such as field emission scanning electron microscopy (FESEM) and HRTEM to characterize the evolutions. Building on this, Lou et al. in 2016 created nitrogen-doped hollow CNT materials (NCNTFs) from ZIF-67 (Fig. 4a–c), finding that optimal structures formed at 700 °C with the morphology of the precursor preserved[108]. The calcination temperature influenced the CNT length, and the presence of hydrogen was crucial for the formation of hollow structures. The ZIF-67 particles served dual roles as a carbon and nitrogen source and as a template, resulting in NCNTFs with superior electrocatalytic activity compared to commercial Pt/C electrocatalysts. In 2017, Wang et al. combined MOF-67 with melamine, using a two-step warming procedure to produce spherical actinide-based carbon nanotube assemblies (3D-CNTA)[109]. ZIF-67 functioned as both a precursor and a structural inducer, while melamine initiated the growth of CNTs (Fig. 4d–f). The 3D-CNTA exhibited excellent electrical conductivity, a high specific surface area (up to 108 $m^2\ g^{-1}$), and a rich porous structure, with each CNT encapsulated by Co@NC core-shell particles, enhancing catalytic activity and stability. Wang et al. also summarized the progress in preparing CNT-based materials from MOFs[55], emphasizing the benefits of using MOFs for CNT growth and the creation of hierarchical CNT structures that traditional methods cannot achieve[110]. The controlled synthesis of CNTs with tailored properties remains an active area of future research.

Our group has also made significant progress in synthesizing CNTs material with tailored structures at relatively low temperatures through a double-temperature zone CVD route (Fig. 5a)[57]. We successfully prepared 3DOM CNT aggregates[57,111], also known as ordered macroporous graphene-like carbon materials (OMGCs)[112], at a annealing temperature of 400 °C. This was achieved using a co-sacrificial hard template composed of Ni salts-impregnated polymethyl methacrylate (PMMA) microspheres. We identified 3 critical parameters that significantly influence the microstructure and morphology of the final material: the

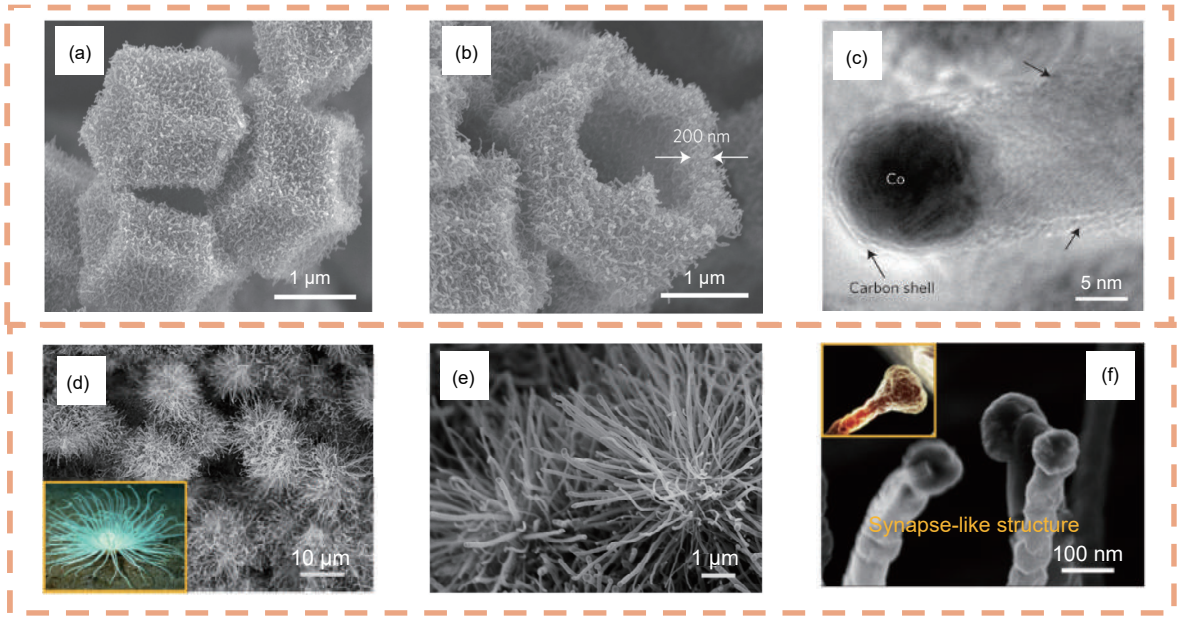

Fig. 4 (a–b) FESEM and (c) HRTEM images of NCNTFs[108]. (d–e) FESEM and (f) HRTEM images of 3D-CNTA[109]. (Reproduced with permission)

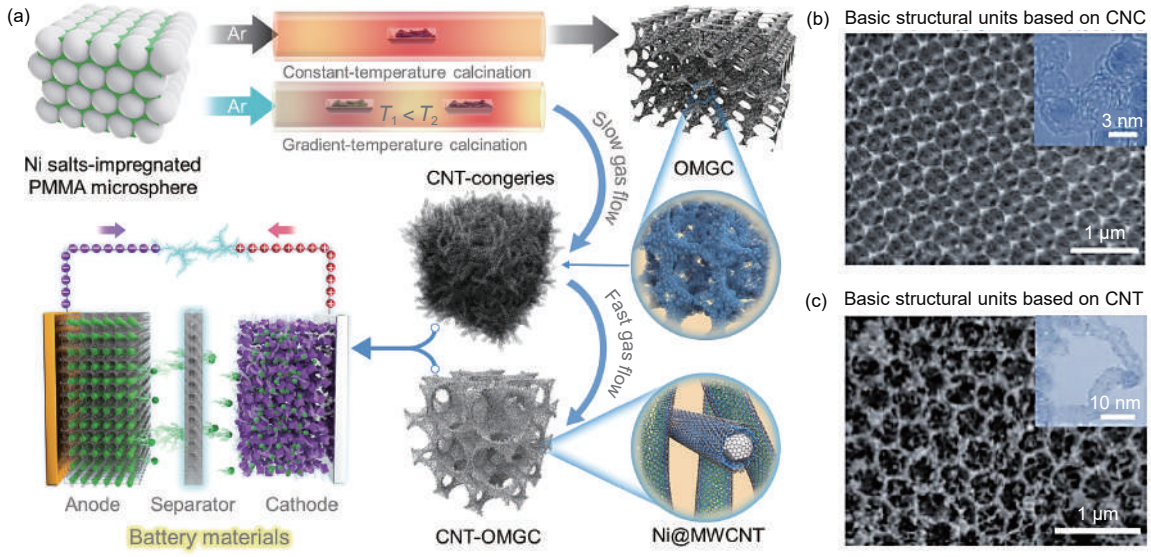

Fig. 5　(a) Schematic diagram of the preparation process of CNC-OMGCs and CNT-OMGCs carbon-based electrode materials based on nickel nitrate and colloidal crystal microsphere templates[57]. (b) SEM and HRTEM images of CNC-constructed CNC-OMGCs[112]. (c) SEM and HRTEM images of CNT-constructed CNT-OMGCs[57]. (Reproduced with permission)

low-temperature zone calcination temperature, the carrier gas flow rate, and the high-temperature zone calcination temperature. This calcination strategy provides a straightforward preparation route for CNTs with specific morphologies, which is essential for cost-effective and large-scale CNT production. We propose that both the carbon nanocages (CNC) (Fig. 5b)[112] and CNTs structural units (Fig. 5c)[57] can serve as fundamental structural and functional units to facilitate ion and electron transport in EES[57,111,112].

A succinct comparison of the principles, key advantages, and disadvantages of different CNT preparation methods can be found in Table 5[57,106,108,109,111–125]. All in all, when considering the application of CNTs in EES, key factors such as electrical conductivity, dispersion, and cost are paramount. These factors are integral to understanding how different CNT preparation methods meet various application demands and the trade-offs inherent in their selection.

Table 5　Comparison of methods for synthesizing CNTs

Preparation methods	Working principles	Advantages	Disadvantages	Products	References
Arc discharge (AD)	Heat graphite rods to over 3000 °C, vaporizing graphite and depositing CNTs in the presence of catalysts like Fe, Co and Ni for SWCNT production.	High-quality SWCNTs, adjustable process parameters	Complex equipment, high cost, easy to wind, challenging separation and purification	SWCNTs, MWCNTs	[113–117]
Laser ablation (LA)	Use high-energy laser on graphite under high temperature and pressure, causing sublimation and CNT generation with catalyst assistance.	High quality SWCNT	High cost, not scalable	SWCNTs	[118–120]
Chemical vapor deposition (CVD)	Introduce gaseous carbon source with carrier gas into the chamber, and CNTs form at 500−1200 °C with catalysts like Fe, Co and Ni.	Adjustable reaction parameters, controllable CNT structure, scalable	Complex catalyst mechanisms and design, high cost, easy to wind	SWCNTs, MWCNTs	[121–125]
MOF-based growth	CNT grow from MOF catalyzed by metals like Fe, Co, Ni or Zn at 430−900 °C.	With MOF serving as both carbon source and catalyst, potential for diverse CNT structures	Limited research, potential production challenges	NCNTs, NCNTFs, 3D-CNTA	[106,108,109]
PMMA microsphere template-based double-zone CVD	Using polymers or other solid or liquid organics as carbon source in the low-temperature zone, the given precursors containing Ni catalyst in the high-temperature region transform into CNT-OMGCs at 400−1000 °C.	Mild conditions, highly controllable, cost-effective, suitable for 3DOM structure, scalable	Early-stage research	CNT-OMGCs aggregates	[57,111,112]

3 Application of CNTs in EES devices

3.1 Application of CNTs in lithium-ion batteries

As mentioned above, LIBs have been extensively utilized in portable electronics and electric vehicles since the 1990s, owing to their excellent stability and high performance[126–128]. The performance of LIBs is significantly influenced by the electrode materials, with CNTs offering enhanced mechanical strength and electrical conductivity due to their intrinsic properties[129]. The integration of CNTs with electrode materials can provide a long-range conductive network, mitigating volume expansion during charging and discharging processes, and leading to the formation of separated network composite materials with improved performances[130].

3.1.1 Anode

Graphite, with its Li-intercalation chemistry, has been the prevalent choice for anode materials in the past decades. However, its theoretical specific capacity of 372 mAh g^{-1} is insufficient to meet the increasing demands for high-performance batteries. Alternative materials with transformation or alloying mechanisms, such as elements from the IVA and VA groups (Si, Sn, Al, Sb, etc.), offer higher theoretical capacities. Yet, these materials contend with challenges including poor electrochemical reversibility and significant volume changes during lithiation and delithiation[131].

To address these issues, the integration of 1D carbon materials into 3D hybrid micro/nanostructures has been explored. This approach can replace traditional pure carbon materials in commercial LIB anodes, leading to improved economics and enhanced performance. For instance, Yan et al. demonstrated the synthesis of CNT-embedded 3D graphite foam using a CVD technique (Fig. 6a)[132]. By using commercial nickel foam as a template and ethylene as a carbon source, they created a 3D graphite structure through a calcination process in a hydrogen-argon atmosphere. The subsequent etching of the nickel template and the growth of CNTs on the resulting graphite foam led to the formation of a composite material. This composite, particularly the well-dispersed carbon nanotube assemblage (G-CNT) obtained through an additional annealing step, showed remarkable electrochemical performance, retaining a capacity of 200 mAh g^{-1} at a high current density of 500 mA g^{-1}.

Si-based anode materials are among the most promising candidates for next-generation LIBs due to their theoretical specific capacity, which exceeds that of commercial graphite by more than tenfold[130]. They also offer a lower voltage platform and are cost-effective due to the abundance of Si reserves[133–136]. Des-

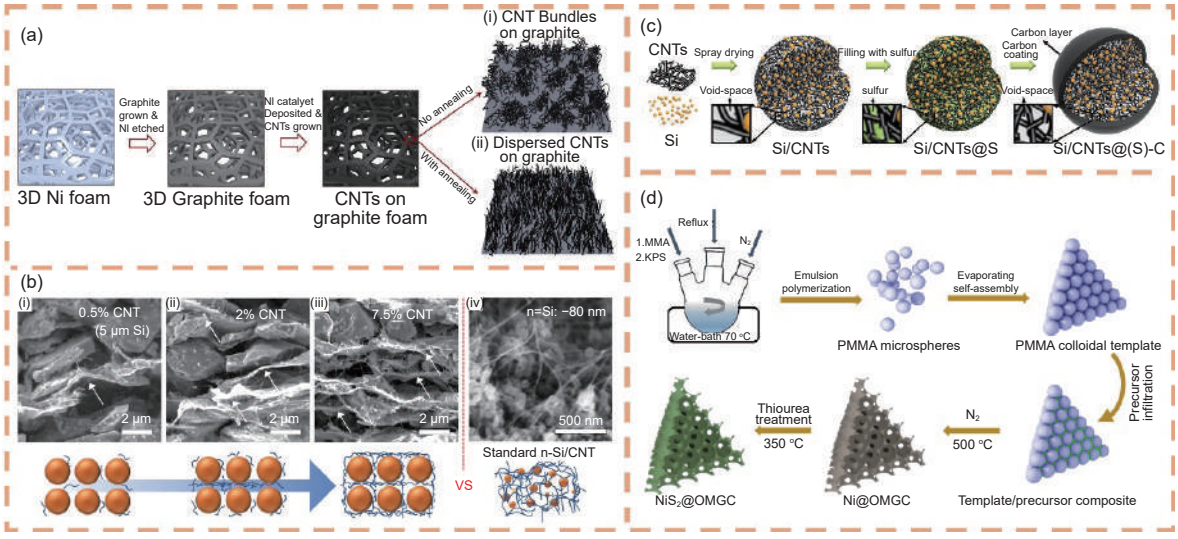

Fig. 6 (a) Schematic illustration of controlled CNT growth on graphite foam[132]. (b) SEM images and schematic diagram of separation network formed between CNTs and silicon as the mass of CNTs increases[145]. (c) Schematic of the Si/CNTs@(S)-C design[146]. (d) Preparation and application diagram of 3DOM NiS_2@OMGC[156]. (Reproduced with permission)

pite these advantages, the development of silicon-based anodes has been slow due to several challenges. The semiconductor nature of Si results in poor electrical conductivity, which hampers ionic conductivity[130,137,138]. Moreover, the substantial volume changes during charging and discharging generate stress that can lead to particle cracking and pulverization, ultimately causing electrode failure[139]. Additionally, these volume fluctuations can result in an unstable solid electrolyte interface (SEI), exacerbating capacity degradation and reversibility deterioration.

To overcome these issues, researchers have developed strategies such as making Si/CNTs composites, nano-sizing silicon, electrode structure design, pre-lithiation, and electrolyte additive engineering[140–144]. Notably, the rational design of Si/CNTs composites has proven effective in addressing these challenges. Park et al. produced Si/CNTs composites using a ball milling method, which significantly improved the electrochemical properties once the CNT content reached optimal levels (Fig. 6b)[145]. This structural design allowed for the fabrication of high-performance silicon-based electrodes with thicknesses up to 300 micrometers, enhancing conductivity and mechanical toughness. Consequently, the Si/CNTs anode material achieved an ultra-high area capacity of up to 45 mAh cm^{-2} in a half-cell, with a full-cell capacity of 29 mAh cm^{-2}, a mass energy density of 480 Wh kg^{-1}, and a volumetric energy density of 1 600 Wh L^{-1}. Zhang et al. introduced a 3D Si/CNTs composite with voids and carbon shells, which demonstrated robust capacity and cycling stability properties (Fig. 6c)[146]. After 1 000 cycles at 0.2 C, the composite maintained a reversible capacity of 943 mAh g^{-1}, and even at varied cycling rates, the electrode's reversible capacity reached 622 mAh g^{-1}.

Despite the progress, the application of CNTs in LIBs remains challenging. The cycle life and safety performance of CNT and microscale Si-based anode composites require further enhancement. Additionally, the fabrication process of Si/CNTs composites is complex and may involve environmentally harmful acid etching[147,148]. Therefore, there is a need to optimize the preparation process, with the potential to use ball milling and spray drying methods to prepare Si-based negative electrodes as a foundation for Si/CNTs composites. The synthesis of Si/CNTs composites is intricate, and achieving industrial-scale production is a goal yet to be realized[126].

Conversion anode materials, which undergo a conversion reaction for lithium storage, typically include transition metal oxides, sulfides, selenides, and nitrides[149,150]. These materials often face issues of volume expansion and low conductivity during charging and discharging. Combining them with highly conductive carbon materials is a viable solution. The performance of electrode materials is influenced not only by their structural units but also by their microscopic morphology[126]. 3DOM materials have gained attention in energy storage due to their larger specific surface area and porous 3D structure[151–155]. Our group's research has explored 3DOM graphenic carbon materials, demonstrating the OMGCs preparation using PMMA microsphere template and a solution of metal nitrate and citric acid[112]. Building on this, Liu et al. created Ni_2S@OMGC composites within a 3DOM carbon matrix, which showed excellent electrochemical Na-storage performance (Fig. 6d)[156]. Wang et al. proposed a self-templated gradient calcination process by CVD to synthesize CNT-OMGCs (Fig. 5a) [57,111], which exhibited a conductivity (~ 1.0 S m^{-1}) approaching that of commercial CNTs. The implementation of these honeycomb-networked carbon materials as conductive additives in LIBs demonstrated superior performance over traditional carbon blacks and many commercial CNTs, underscoring their substantial potential for applications in the EES sector.

3.1.2　Cathode

Initially, LIBs employed lithium cobalt oxide ($LiCoO_2$) as the layered oxide cathode material. However, its relatively low theoretical specific capacity did not meet the evolving demands for high energy density, long cycle life, and a wide application temperature range. Consequently, research has led to the discovery of alternative cathode materials, includ-

ing lithium manganate spinel ($LiMn_2O_4$), lithium iron phosphate ($LiFePO_4$, abbreviated as LFP) with an olivine structure, and layered ternary oxides ($LiNi_xCo_yMn_2O_2$, shorted as NCM111, NCM523, NCM811), which have achieved higher energy densities[157]. Despite these advancements, these materials grapple with challenges such as poor electrical conductivity and suboptimal cycling stability. As analyzed, the integration of CNT materials with cathode active materials can significantly boost their performances[155].

$LiMn_2O_4$, a spinel compound with charging and discharging voltages between 3.5 and 4.3 V and a theoretical specific capacity of 148 mAh g^{-1}, has been utilized in the development of $LiMn_2O_4$/CNTs and $LiNi_{0.5}Mn_{1.5}O_4$/CNTs composites by Le et al.[158]. These nanocomposite cathode materials exhibited greater efficiency for Mn^{3+}/Mn^{4+} and Ni^{2+}/Ni^{4+} redox pairs, positioning them as promising candidates for high-power lithium secondary batteries. Guo et al. leveraged the high electronic conductivity and large aspect ratio of SWCNTs as a conductive agent to fabricate a self-supported ultra-thick $LiMn_2O_4$@CNTs material with a thickness of up to 600 μm, a loading of approximately 190 mg cm^{-2}, and an areal capacity of 20 mAh cm^{-2}[159]. This exceeded the thickness and loading capacity of conventional materials. The SWCNTs formed an intertwined yarn structure on the $LiMn_2O_4$ surface, endowing the electrodes with robust mechanical strength and flexibility. Notably, these electrodes remained intact without cracks even after a 180° bend. Electrochemical tests revealed that the electrode with a mass loading of 30 mg cm^{-2} retained 94% of its capacity after 50 cycles at 0.5 C, while the 60 mg cm^{-2} electrode showed a capacity retention of 95% after 50 cycles at 0.1 C. The 190 mg cm^{-2} ultra-thick electrode (600 μm) boasted a remarkable areal capacity of 20 mAh cm^{-2} with 97.5% (mass fraction) active material, underscoring the benefits of SWCNTs' exceptional electrical conductivity (Fig. 7a)[159].

$LiFePO_4$ (LFP), an olivine-structured material, is widely used as a cathode material in LIBs due to its high theoretical specific capacity, long cycle life, abundance, low cost, and environmental friendliness[160]. However, its low electronic conductivity and sluggish Li^+ diffusion impede its broader application[161]. To address this, high conductivity material modifications have been explored to achieve high energy and high power performances[162]. Gao et al. utilized co-precipitation and microwave plasma CVD (MPCVD) techniques to prepare a LFP/CNTs nanocomposite. SEM observations indicated that the particle size of the LFP/CNTs nanomaterials decreased post-composite formation (Fig. 7b, c)[163]. The MPCVD method prevents particle growth, and the CNTs' presence inhibits LFP particle aggregation. The nanocomposites consist of LFP nanoparticles encapsulated by curled CNTs, forming an effective 3D conductive network that connects individual LFP nanoparticles. HRTEM images revealed the clear lattice structure of LFP, with lattice stripes of 4.27 Å width corresponding to the (101) face of the orthorhombic phase. Electrochemical kinetic studies attributed the enhanced performance to the swift transport of ions and electrons, with uniform distribution of electrons and ions throughout the nanocomposites.

LFP has been extensively used in electric and hybrid electric vehicles due to its superior cycling stability[164]. However, high-rate Li^+ transport is limited, potentially due to restricted Li^+ transport near the active site in the electrolyte, crucial for fast charging[165]. To modify LFP materials, Wang et al. introduced a design involving the in-situ embedding of CNTs during a hydrothermal process to decorate porous LFP microspheres[166]. This dual-carbon modified porous structure, named C@LFP/CNTs (Fig. 7d)[166], improved the transport kinetics of electrons and Li^+ ions, achieving high bulk energy density, excellent rate performance, and stable cycling performance. The C@LFP/CNTs maintained a specific capacity of 73 mAh g^{-1} at a high rate (60 C) and retained a reversible capacity of 113 mAh g^{-1} after 1 000 cycles at 10 C, with a capacity retention of 98%. For fast charging, the material's performance was evaluated by charging at 20 C and discharging at 1 C. The char-

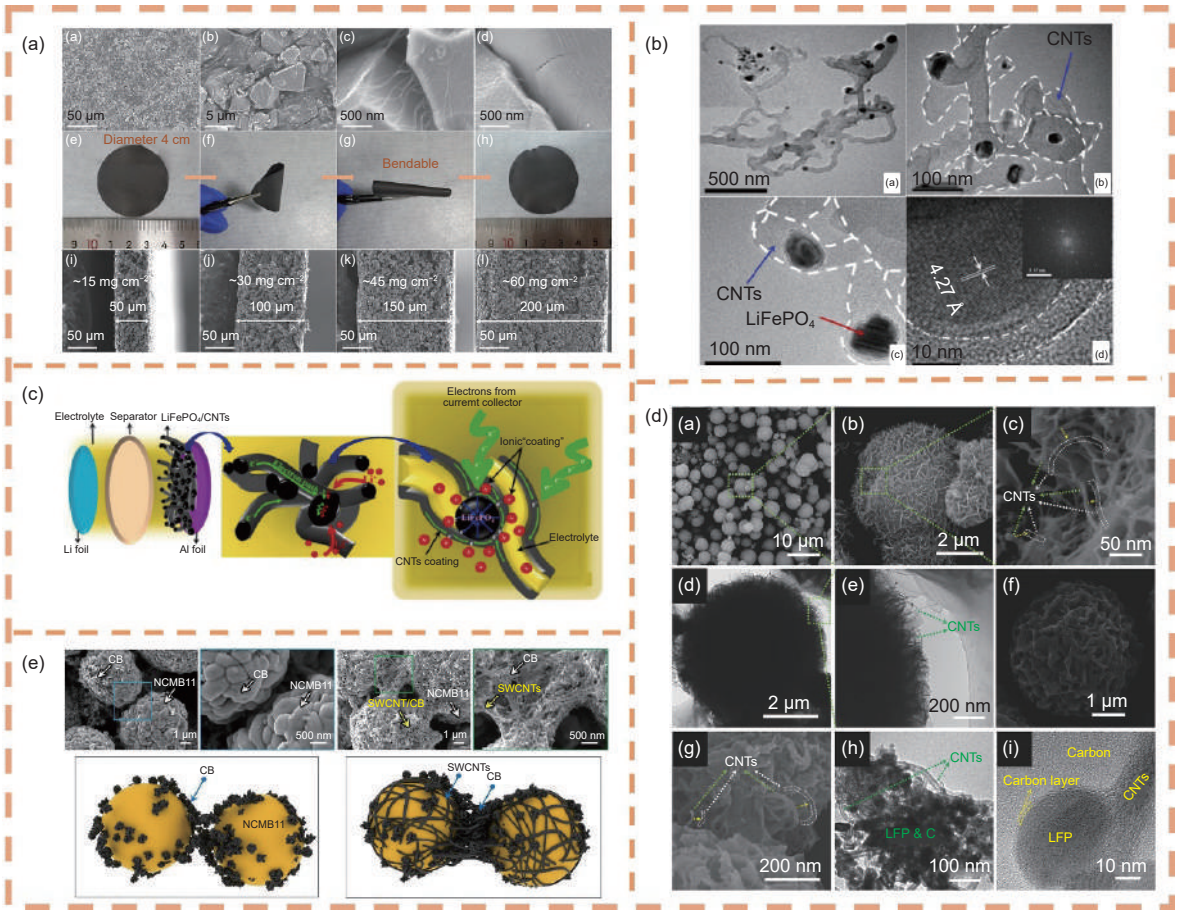

Fig. 7　(a) Morphology characterizations of F-LMO electrodes[159]. (b) TEM images of $LiFePO_4$/CNTs nanocomposites[163]. (c) Schematic diagram of electrode process dynamics: electrons and ions distribute uniformly in the $LiFePO_4$/CNTs nanocomposites[163]. (d) SEM, TEM and HRTEM images of C@LFP/CNTs[166]. (e) Schematic structure and the electronic photo of the electrical pathway formed by NCM-CB and NCM-SWCNT[168]. (Reproduced with permission)

ging process took 142 s, achieving a charging capacity of 117 mAh g^{-1} (76% of the total capacity). After 200 s of charging (including 142 s of galvanostatic current charging and 58 s of galvanostatic voltage charging), the total charging capacity reached 135 mAh g^{-1}, with a charging efficiency of about 90%, surpassing some industry standards (80% charging efficiency in 30 min). The volumetric energy density of C@LFP/CNTs-based LIB was also evaluated, maintaining a volumetric energy density of 443 Wh L^{-1} at 10 C, which is one-third higher than that of commercial LFP/C (323 Wh L^{-1}). Even at current rates up to 60 C, a high volumetric energy density of 219 Wh L^{-1} can be achieved, highlighting the potential of C@LFP/CNTs for advanced EES and conversion devices in electric and hybrid electric vehicles.

In comparison to LFP materials, layered ternary oxide cathode materials such as NCM111, NCM523 and NCM811 can achieve higher energy density due to their higher charging platforms and cut-off voltages[167]. SWCNTs, with their excellent electrical conductivity, can enhance the electrochemical performance of ternary anodes when dispersed effectively. However, their large bundle size makes dispersion challenging, limiting their application in energy storage. Kim et al. introduced a method for dispersing SWCNTs using strong acid and co-co-solvent ($NaNO_3$) for mild oxidation, which improved the dispersion from liquid crystal slurry and was used as a conductive agent in LIBs[168]. The resulting 15 μm CNT film exhibited a conductivity of 2.3×10^5 S m^{-1}, outperforming traditional carbon black electrodes (Fig. 7e)[168]. The cathode with SWCNT conductive agent material showed better structural integrity and a capacity retention rate of 83% after 100 cycles at 1 C, 23% higher than that of carbon black. While SW-

CNTs offer superior performance, their high cost is a drawback. MWCNTs are more cost-effective and widely used. Kim et al. reported a 3D MWCNTs hybrid that cladded the surface of NCM523 material, with a capacity retention of 94% after 300 cycles of cycling tests at 1 C[155]. This indicated that physical surface coating of CNTs can improve performance to a certain extent but may result in poor coating uniformity. Qu's research group found that coating NCM811 anode with Mg-Al layered double oxide (Mg-Al-LDO) could enhance cycling stability and increase reversible specific capacity by 5%[169]. Furthermore, the group investigated NCM811 microspheres with 3D hierarchical composite interconnects made from 2D Ni-Al LDO flakes and 1D CNTs (named LDO&CNT), which improved the cycling and rate performance of LIBs. The analysis showed that the high conductivity of CNTs, interconnected with Ni-Al LDO nanosheets, not only prevented CNT aggregation and Ni-Al LDA sheet stacking but also accelerated Li^+ and electron shuttling between the electrolyte and electrode materials, reducing electrochemical polarization.

Since the inception of LIB systems, the incorporation of CNTs has been shown to enhance electronic conductivity, improve Li^+ diffusion, maintain material morphology stability, and increase reversible capacity, rate capacity, and cycling stability. Nonetheless, the synthesis of CNT-based nanocomposites faces several challenges, including poor adhesion of nanoparticles to CNTs, difficulty in achieving homogeneous dispersion, the need to minimize CNT content without causing particle agglomeration, and the high cost of SWCNTs[163]. Additionally, the development of environmentally friendly, low-cost process technologies for high-volume synthesis and fabrication of nanocomposites is essential[157]. It is important to note that while current research often focuses on the electrochemical performance of CNTs, their safety in battery-level systems is an area that requires more attention[126].

3.2 Application of CNTs in lithium-metal batteries

As discussed above, LIBs are extensively utilized in electronic products and electric vehicles due to their high energy density, excellent electrochemical properties, and superior cycle stability. However, the increasing demand for new energy devices is outpacing the capabilities of the current LIB system. The next generation of high-energy-density energy systems, which exceed 350 Wh kg^{-1}, has surpassed the traditional graphite-based LIBs. LMBs, with their lowest electrochemical potential of –3.04 V compared to standard hydrogen electrodes and an ultrahigh theoretical specific capacity of 3 860 mA h g^{-1}, are considered the most promising battery systems for the future and have garnered extensive research attention[6].

Nonetheless, like a coin with two sides, LMBs, despite their aforementioned advantages, face significant challenges[170]. Firstly, Li metal is highly reactive and prone to side reactions with the electrolyte solution, leading to the formation of a SEI film. While the SEI film facilitates the passage of Li^+ ions, it is not conductive to electrons. Moreover, the SEI film is unstable and can be damaged during the repeated cycles of charging and discharging, consuming additional electrolyte[171]. The instability of the SEI film can result in non-uniform local current densities, affecting the uniform Li deposition and ultimately leading to the formation of Li dendrites, which significantly impact the battery's Coulombic efficiency[172].

In the LMB system, key parameters such as Li nucleation overpotential, Coulombic efficiency, and cycle stability are crucial. These parameters are intrinsically linked to the battery's electrochemical reactions, involving Li^+-electron transport speeds and interface stability. Advanced characterization techniques have enabled researchers to delve deeper into the mechanistic aspects of LMBs, fostering rapid advancements in the field[172].

To address the challenges of LMBs, researchers have employed several strategies to enhance their electrochemical performance. One approach involves the design of an artificial SEI layer to protect the lithium metal and reduce side reactions with the electrolyte[173,174]. Another promising method is the use of 3D

collectors, including 3D copper[175] and various carbon materials[176], to mitigate volume changes during the charging and discharging processes. Carbon materials offer a natural advantage in LMBs due to their lightweight nature, high electrical conductivity, and adjustable structures. However, the poor lithophilicity of carbon materials can lead to high local current densities and limited Li deposition, potentially causing Li dendrite formation and safety issues[177]. To counteract this, lithophilic materials such as metal oxides, metal nitrides, nano-metal particles, and heteroatom-doped materials have been incorporated into the carbon matrix[6,129,177]. Pre-lithiation is also used to deposit some Li, which facilitates further Li deposition.

CNT materials hold great promise in LMB systems due to their lightweight nature, high conductivity, large specific surface area, and hollow inner cavity structure, which can effectively reduce local current density[178–180]. For instance, Wan's group prepared a CNT paper by self-assembly using MWCNTs and used it as a scaffold for the anode of LMBs (Fig. 8a)[179]. The cell achieved an ultra-high area capacity of 10 mAh cm^{-2} and a specific capacity of 2 830 mAh g^{-1}, maintained over 1 000 cycles at 10 mA cm^{-2}, avoiding Li dendrite formation and battery short-circuiting. The CNT paper is lightweight, robust, and scalable, capable of withstanding large volume changes and ensuring the integrity of the microcircuits within the electrodes during Li stripping/plating cycles. Yang et al. utilized commercial CNTs as self-supporting substrates for Li metal (Fig. 8b)[180]. The porous structure allows Li to deposit on the porous sites, forming a pre-lithiated substrate that induces uniform Li deposition. Chung's research team investigated the impact of a 3D conductive network structure, created by combining CNTs and graphene, on the electrochemical performance of LMBs (Fig. 8c)[181]. They found that a CNT to graphene ratio of 25∶75, used as a Li substrate, could exhibit enhanced rate performance and extended cycle life. Additionally, when CNTs were used as the positive electrode in lithium-sulfur batteries (LSBs), an optimal ratio of 50∶50 was found, allowing for 200 cycles at 0.1 C with a capacity retention rate of 60%. Chen's group designed a 3D NiO/CNT material by incorporating NiO into CNTs, which showed excellent affinity for molten Li, inhibited Li dendrite formation, and exhibited excellent electrochemical performance[182]. The NiO, a lithophilic material rich in nucle-

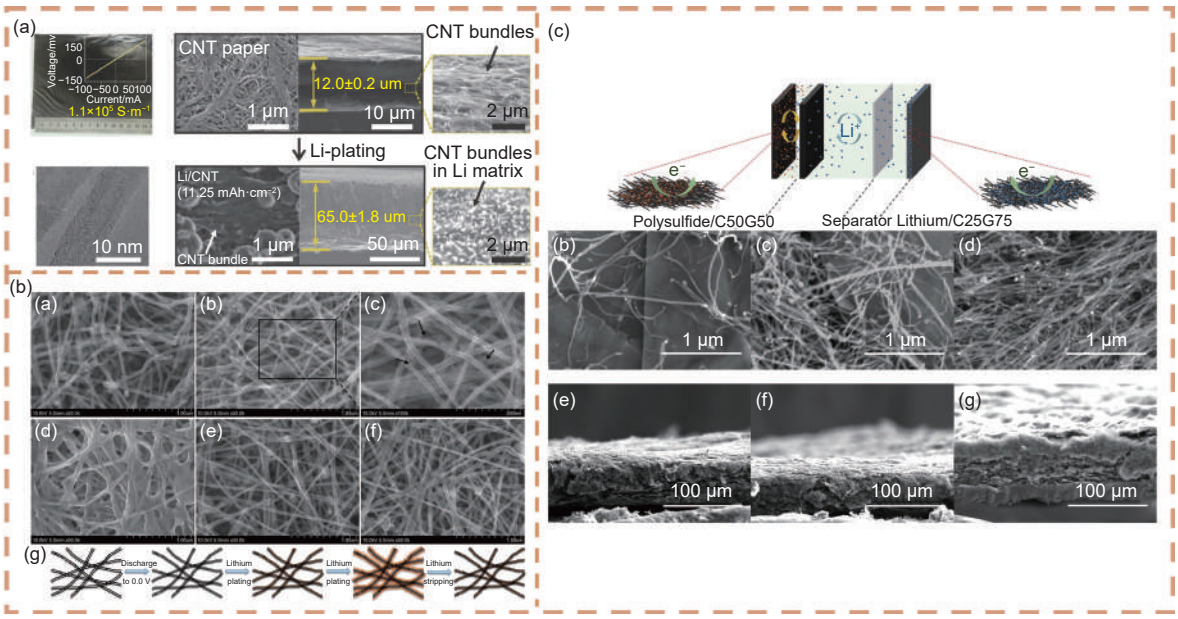

Fig. 8　(a) Characterization of the CNT paper and the Li/CNT electrode with Li loading of 11.25 mAh cm^{-2}[179]. (b) Morphologies of the CNT sponge at different stages of lithium plating and stripping[180]. (c) Illustration of the carbon structural materials in a lithium-sulfur cell and the material characteristics of the carbon structural materials with different ratio of CNT and graphene[181]. (Reproduced with permission)

ation sites, contributed to the homogeneous Li deposition. The CNTs' outstanding electrical conductivity and large specific surface area reduced localized current density and individual Li formation. The symmetric cell assembled with this material could operate stably for 900 h with an overpotential potential of only 30 mV. When paired with LFP, the full cell exhibited a specific capacity of 140 mAh g^{-1}. Tan et al. modified CNTs with manganese dioxide (MnO_2), which provided lithophilic and dendrite-free surfaces[183]. The MnO_2-modified CNTs demonstrated excellent performance, with a lifetime of over 1 800 h and an area capacity exceeding 10 000 mAh cm^{-2} when Li plating and stripping were repeated at a high areal capacity of 6 mAh cm^{-2}. The significant improvement is attributed to the highly conductive porous CNT framework, the low overpotentials due to the excellent Li affinity and electrolyte wetting properties of MnO_2, and the mossy structure with a large surface area and distributed Li insertion into MnO_2/CNT, which inhibits dendrite formation.

Despite the progress made in Li-carbon composite anode materials, the practical application of LMBs still faces considerable challenges, particularly regarding high energy density and safety issues related to Li metal itself. Future research should focus on several key areas[184]: (1) Elucidating the working principles of Li metal batteries through theoretical simulations and advanced characterization techniques; (2) Emphasizing the design of Li-carbon composite anodes with a focus on high current density, extended cycle life, and high Coulombic efficiency; (3) Exploring the constitutive relationship between carbon-based substrates and lithophilic materials to enhance LMB performance; (4) Combining multiple strategies to improve the safety and cycling performance of LMBs, as a single approach may have limited impact.

3.3 Application of CNTs in lithium-sulfur batteries

LSBs, a variant of LMBs as discussed earlier, boast an impressive mass energy density of 2 600 Wh kg^{-1}. The use of sulfur, which is naturally abundant and low in toxicity, offers potential economic and environmental advantages, making the LSB system one of the most promising EES technologies[185]. However, LSBs face several challenges due to the insulating nature of sulfur cathode and its discharge products (Li_2S_2, Li_2S), the shuttling of polysulfide intermediates between the electrodes, the volumetric expansion of sulfur during cycling, and the corrosion of Li metal surfaces. These factors contribute to high self-discharge, low capacity reversibility and a short cycle life[186]. To develop LSBs with the desired energy densities, the electrode materials should possess specific properties[186], such as a large pore volume to accommodate a high content of active materials, good electrical conductivity to ensure efficient utilization of sulfur, and large particle sizes to minimize the use of binders and conductive carbon additives, with binder-free electrodes being the ideal goal. Furthermore, research into separators and electrolytes is crucial for achieving high-performance LSBs[187–190]. This subsection will expand on the above points, discussing the modification of LSB separators with CNTs, and the application of CNTs in cathode materials of LSBs.

3.3.1 Intermediate layer material based on separator modification

To address the challenges inherent in LSBs, various nanostructured carbon materials have been explored as interlayer materials of seperators. CNTs, with their distinctive 1D nanostructures, have been particularly noteworthy for their exceptional flexibility, electrical conductivity, and chemical stability. They have been integrated into the interlayer of LSBs to inhibit the shuttle effect of lithium polysulfides (LiPSs)[190]. MWCNTs are preferred over SWCNTs due to their lower preparation cost and simpler synthesis conditions, as well as their high electrical conductivity, low thermal expansion coefficient, and structural stability[191]. MWCNTs serve dual roles in the intermediate layer of LSBs, i.e., as a coating for the separator or self-supporting membrane[192].

Separators are essential components in LSBs that isolate the positive and negative electrodes to prevent internal short circuits. However, the pore size of com-

mercial separators, approximately 100 nm, is relatively large, which is insufficient to confine polysulfides effectively[193]. This allows soluble LiPSs to migrate to the negative electrode under the influence of a concentration gradient during sulfur reduction and to the positive electrode during oxidation, driven by the electric field, leading to a pronounced shuttle effect.

To curb the shuttling of dissolved LiPSs, a variety of MWCNT-based materials have been engineered to modify the separators, offering both physical trapping and chemical adsorption of LiPSs, thereby enhancing the electrochemical performance of LSBs[194]. MWCNTs are extensively used to coat LSB separators. For instance, Chung and Manthiram developed MWCNT-coated separators that effectively anchor dissolved LiPSs[195] (Fig. 9(a, b)). The MWCNT layer facilitates fast electron transport and high sulfur utilization while also acting as a filter to trap and adsorb LiPSs. The porous structure of the MWCNT layer also promotes electrolyte permeation and electron/ion diffusion. Batteries with MWCNT-coated separators exhibit enhanced long-cycle performance, with specific capacities of 881, 809 and 798 mAh g^{-1} after 150 cycles at 0.2, 0.5 and 1 C, respectively. Additionally, Ponraj et al. synthesized hydroxyl-functionalized CNTs (denoted as CNTOH) encapsulated on the separator (Fig. 9c)[196]. Leveraging the good conductivity and polarity of CNTOH, this modification can address the issue of poor conductivity of the active substance and mitigate the diffusion and migration of LiPSs in LSBs, further improving the battery's performance and stability.

Metal-based compounds, including metal oxides, sulfides, phosphides, borides, hydroxides and MOFs, can interact chemically with LiPSs through polar interactions, thus inhibiting their shuttling in LSBs[197]. For example, the Ce-MOFS/MWCNTs composite prepared by Hong et al., achieved an initial specific capacity of 993.5 mAh g^{-1} at 0.1 C with a high sulfur loading of 6 mg cm^{-2} when used as a coating for the Li-S battery separator (Fig. 9d)[198]. After 200 cycles, the battery retained an impressive capacity of 886.4 mAh g^{-1}. The uniform distribution of catalytic active centers, large specific surface area, and good

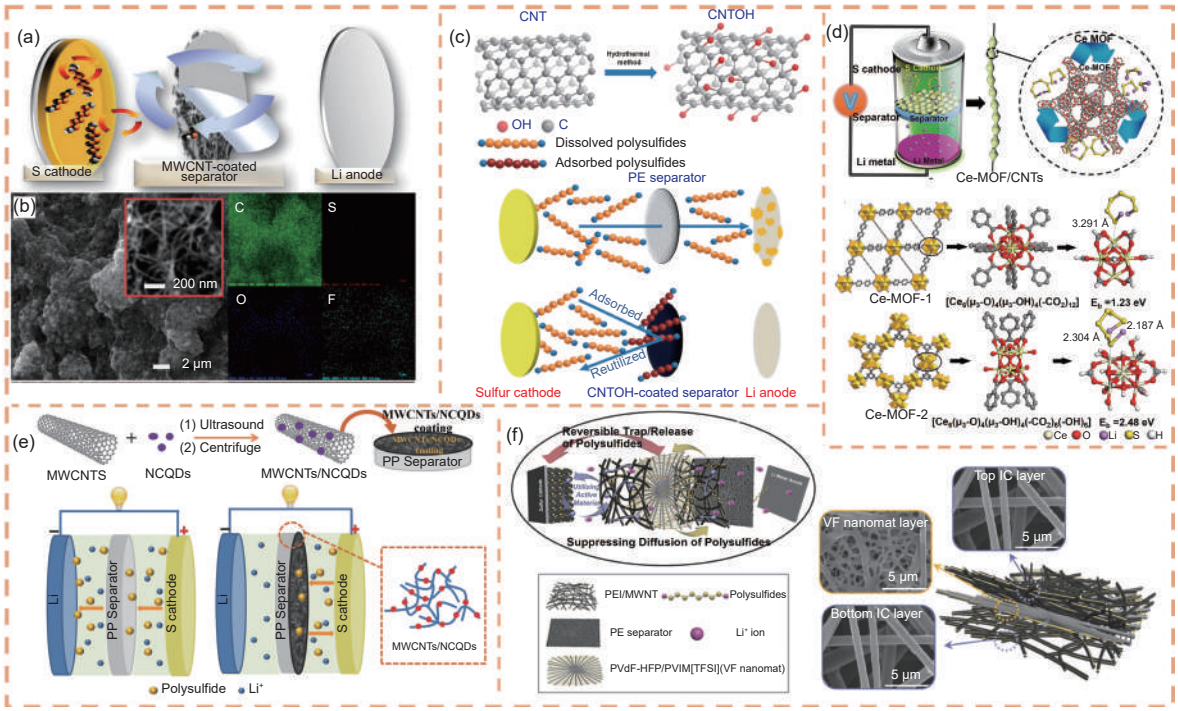

Fig. 9　(a–b) Mechanism and SEM image of MWCNTs-coated separator for LSBs[195]. (c) Schematic illustration of trapping LiPSs by the CNTOH-coated separators[196]. (d) Scheme of Ce-MOFs/CNTs as coating materials in LSB and the Li_2S_6 adsorption sites in the Ce-MOF[198]. (e) Schematic diagram of MWCNTs/NCQDs-coated separator preparation process and the application in LSBs[200]. (f) Application of spiderweb separator in LSBs and the corresponding SEM images[201]. (Reproduced with permission)

electronic conductivity of Ce-MOFS/MWCNTs contribute to their excellent electrochemical performance, mitigating the transport and diffusion of polysulfides and promoting the efficient catalytic conversion of LiPSs. Yao et al. combined 2D antimony sulfide (Sb_2S_3) flakes with MWCNTs (Sb_2S_3/MWCNTs) to enhance the Celgard polypropylene (PP) separator[199]. The low average capacity decay rate of LSBs with Sb_2S_3/MWCNTs-modified separators (~ 0.049% after 1 000 cycles at 1 C) indicates a strong interaction with polysulfides, as confirmed by density functional theory (DFT) calculations.

The synergistic effects of different components in nanocomposites typically result in superior properties compared to single-component materials, attracting significant research interest[193]. MWCNT-based composites, such as MWCNTs/carbon, MWCNTs/polymer, and MWCNTs/metal matrix composites, have been extensively utilized as coatings for LSB separators. Pang et al. prepared MWCNT/N-doped carbon quantum dots (NCQDS) composites for this purpose (Fig. 9e)[200]. The large specific surface area and abundant oxygen-containing functional groups of CNTs make them effective adsorbents for LiPSs and contribute to the enhanced electrical conductivity of the composites. Batteries with MWCNT/NCQDS-coated separators show improved electrochemical performance, with an average self-discharge rate of about 11% after 48 h, lower than that of cells with unmodified MWCNT separators.

In addition, scholars have prepared MWCNTs/polymer composites to capture LiPSs in LSBs through physical blocking and chemical bonding strategies. For example, a spider web diaphragm consisting of three functional nanomaterials with good mechanical properties and excellent electrical conductivity was developed. (Fig. 9f)[201]. When it was tested in a LSB's separators, the cell had a higher discharge capacity and more stable cycling performance than those with polyethylene (PE) separators.

3.3.2 Self-supporting intermediate layer material

Beyond the use of MWCNT-based materials to coat the separator to curb LiPSs shuttling, an alternative strategy involves inserting a self-supporting sandwich layer between the cathode and the separator[202]. These self-supporting interlayers are typically thicker than modified separators and exhibit strong chemical and/or physical adsorption capabilities for polysulfides, ensuring effective interaction. Additionally, the interlayer should permit unhindered diffusion of Li^+ ions while preventing the passage of LiPSs on the cathode side[203].

Graphene oxide (GO) has garnered increased interest in EES due to its rich oxygen functional groups, substantial specific surface area, and excellent electrical conductivity[204]. In the context of LSBs, numerous studies have explored the combination of MWCNTs with GO to form barrier materials that inhibit the shuttling of LiPSs. Kim et al. synthesized a freestanding GO/MWCNTs thin film[205], which demonstrated high electronic conductivity and a robust ability to anchor LiPSs, thereby enhancing the electrochemical performance of LSBs. The battery utilizing the GO/MWCNTs film delivered an initial specific capacity of 1 370 mAh g^{-1} at 0.1 C, and after 300 cycles at 0.2 C, it maintained a discharge specific capacity of 671 mAh g^{-1}, corresponding to a capacity decay rate of approximately 0.043% per cycle. Wu et al. introduced a 3D graphene/MWCNTs aerogel (G/MWCNTs) as a self-supporting interlayer to further improve the performance of LSBs[206]. This aerogel, with its 3D interconnected porous network, was fabricated through the rapid reduction of a graphene/MWCNTs aerogel by self-propagation combustion. The G/MWCNTs aerogel possesses good mechanical elasticity and numerous pore channels, which safeguard the integrity of the intercalation layer during battery assembly and provide ample active centers for anchoring LiPSs.

Despite the significant enhancement in the electrochemical performance of LSBs with CNTs-based interlayers, unresolved issues remain before practical application can be realized[193]. While CNTs materials aid in anchoring LiPSs, they only partially address the shuttle effect from either a physical or chemical perspective[207]. The active material can still migrate to

the negative side during cycling. Moreover, in most of the aforementioned studies, the sulfur loading is typically around 1–2 mg cm^{-2}, with the highest not surpassing 10 mg cm^{-2}[208]. As sulfur loading increases, the issues of active material loss and LiPSs shuttling persist despite the presence of a cut-off layer[8]. There is an urgent need to develop new materials with stronger binding energy and interaction with LiPSs. Furthermore, the mechanisms of CNTs-based materials in the loading and catalytic conversion of LSBs, as well as their phase-transition mechanisms during cycling, require more in-depth investigation[209]. Studies on the application of CNTs-based composite interlayers to anodes are scant, necessitating further research in this area. The introduction of a coating or an independent intermediate layer increases the inactive weight ratio of the cell, making it crucial to balance the CNTs interlayer with the overall energy density of the battery for the development of high-energy LSBs[210].

3.3.3　Application of CNTs in positive electrodes

Sulfur is the predominant cathode material in LSB due to its high theoretical capacity. Nonetheless, the intrinsic poor conductivity of sulfur and its discharge products Li_2S_2 and Li_2S, along with the shuttling of soluble polysulfides between electrodes, pose significant challenges[211]. To address these issues, numerous solutions have been proposed, including the integration of sulfur with various conductive carbon-based materials and the introduction of catalytic materials such as transition metal oxides, phosphides, and selenides to facilitate the redox reaction process[193].

A variety of carbon materials have been developed to enhance the electrochemical performance of LSBs, significantly increasing the specific capacity of sulfur and extending the charge-discharge cycle life[209]. One effective strategy is the impregnation of sulfur into conductive porous carbon matrices to form nanostructured composites[212,213]. These materials provide limited space to restrict the diffusion of LiPSs and accommodate the volume expansion of sulfur during cycling[214]. Various carbon materials, including porous carbon particles[215], CNTs[216], CNFs[217], graphene[218], have been explored, with the potential to increase the specific capacity of LSBs to over 1 000 mAh g^{-1}.

Amir et al. developed sulfurized polyacrylonitrile (SPAN) self-supported thin film composites with CNTs as the conductive backbone[219], using a process involving electrostatic spinning and sulfurization (Fig. 10a). By co-spinning sulfur, polyacrylonitrile (PAN), and CNT precursors into nanofibers and vulcanizing them in an elevated temperature sulfur atmosphere, the authors synthesized SPAN-CNT composites with varying CNT to PAN ratios. The addition of 5%–10% CNT to the electrospinning precursor resulted in swollen nanofibers with increased diameter and a roughened surface. An optimal mass ratio of CNT to PAN of 20% was found, with the SPAN-CNT cathode exhibiting a stable discharge capacity of 1 314 mAh g^{-1} and a Coulombic efficiency approaching 100% after 250 cycles at 0.5 C, indicating promising potential for high-performance LSB applications.

While the combination of conductive carbon-based materials with sulfur can improve the electrochemical performance of LSBs, the interaction between carbon materials and LiPSs is primarily through physical adsorption, which is limited. To more effectively anchor LiPSs, the introduction of chemical bonding with polar materials has been explored. Researchers have recently incorporated "strong chemical affinity" into the design of matrix materials to further mitigate the shuttle effect[193].

Wang et al. reported on the growth of MoS_2-MoN heterostructure nanosheets on nitrogen-doped CNT arrays, which were utilized as a freestanding cathode for LSBs (Fig. 10b)[220]. The MoS_2-MoN heterostructure was obtained through a hydrothermal method, with MoS_2 nanosheets grown on CNT arrays and subsequently reduced in a mixture of Ar and NH_3. The MoN component acts as an electron provider to accelerate the redox reaction of LiPSs, the MoS_2 layer ensures smooth Li^+ diffusion and CNT has excellent conductivity. The cathode exhibited excellent cycling performance, with a low capacity decay rate

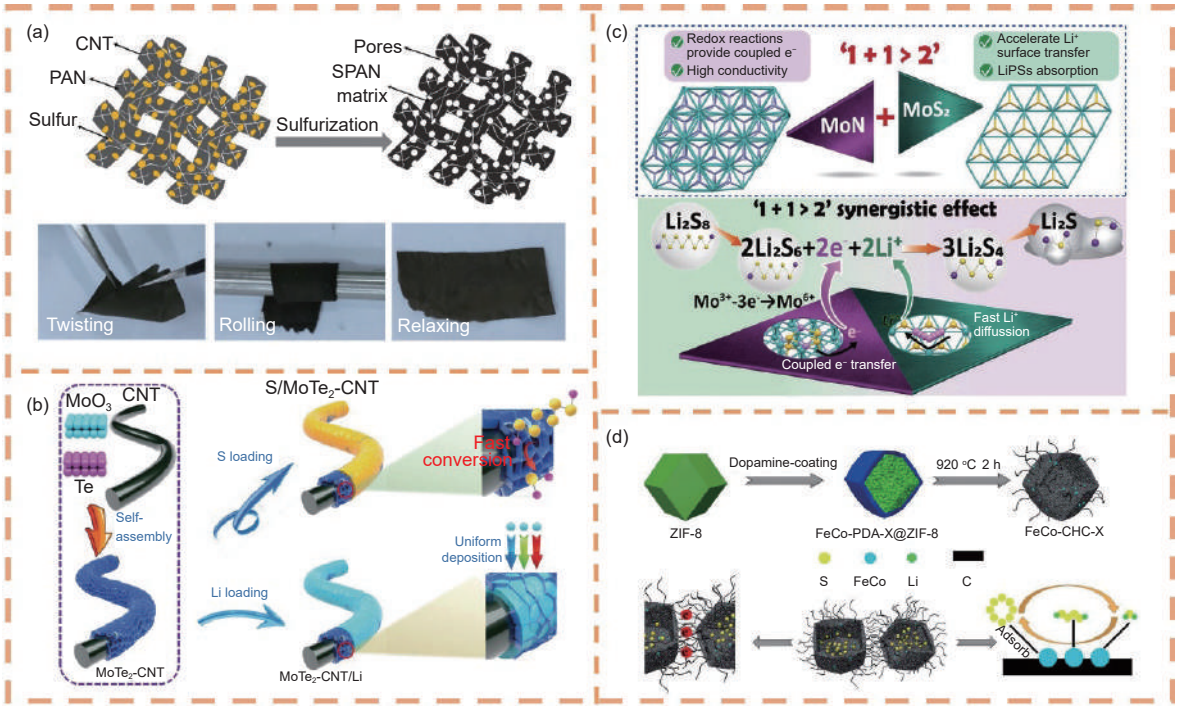

Fig. 10 (a) Schematic illustration and photographs of the flexible SPAN-CNT films[219]. (b) Schematic of the synthesis route for S/$MoTe_2$-CNT and $MoTe_2$-CNT/Li[220]. (c) Schematic illustration of synergistic catalytic of the heterostructure MoS_2-MoN host[221]. (d) Preparation processes of FeCo-CHC-X hosts material[222]. (Reproduced with permission)

of 0.039% per cycle over 1 000 cycles at 1 C and a high initial areal capacity of 13.3 mAh cm^{-2} at an electrolyte volume/sulfur loading ratio (*E*/*S*) of 6.3 mL g^{-1}.

He's group introduced a bifunctional, flexible framework material with metallic 1T-$MoTe_2$ nanosheets grown in situ on CNTs ($MoTe_2$-CNT) (Fig. 10c)[221]. The $MoTe_2$-CNT composite demonstrated the ability to guide homogeneous Li growth and form a sulfide-rich SEI that stabilizes Li deposition, inhibits electrolyte decomposition, and prevents Li loss, thereby extending the cycle life. The full coin cells, with a low negative-to-positive capacity ratios of ca. 2.5 and a high areal capacity of 7.6 mA h cm^{-2}, showed 75% capacity retention after 500 cycles. And, flexible pack batteries fabricated with $MoTe_2$-CNT delivered a high capacity of 1 533 mA h g^{-1} with an energy density of 319 Wh kg^{-1} at a low electrolyte-to-capacity ratio (≈ 2.9 μL/mAh) and a low *E*/*S* ratio (≈ 4.5 μL/mg).

A FeCo alloy modified and CNT linked hollow CNCs host (named CoFe-CHC-X) from Yu's group is constructed by in-situ transformation of Fe and Co elements doped Zn-based MOFs and melamine (Fig. 10d)[222]. The hollow CNCs linked by CNT can facilitate the transport of electrons on the cathode and the physical adsorption of Li_2S_n, promoting the electrochemical performance of LSBs.

It must be emphasized that while scientific research has significantly improved the modification of LSBs, leading to enhanced reversible specific capacity and cycling stability, practical applications still face challenges. These include achieving high sulfur content (> 90%, mass fraction) and high sulfur loading (> 5 mg cm^{-2}), in addition to the previously discussed low *E*/*S* ratio[223].

In the domain of CNT-sulfur composite cathodes, substantial research has been documented. For instance, Li et al. proposed a theoretical model[224] to demonstrate the influence of CNTs on the sulfur content in CNT-sulfur composites, as follows:

$$S\% = \frac{\rho_S \times (4a^2 + 4ad)}{\rho_{CNT} \times d^2 + \rho_S \times (4a^2 + 4ad)}$$

where, ρ_{CNT} denotes the real density of CNTs, typically 1.2 g cm^{-3}, ρ_S is the density of sulfur, with a typical value of 2.07 g cm^{-3}, and a signifies the thickness

of sulfur on the CNT surface, assuming a core-shell structure. The model indicates that the CNT diameter significantly influences the sulfur content in the composite; for example, a CNT diameter of 4 nm can increase the sulfur content to 90% (mass fraction), compared to 54% with a diameter of 20 and 3 nm.

Building on this theory, this research group has developed a sulfur-carbon composite cathode using SWCNTs with diameters of approximately 2−3 nm. Remarkably, with a sulfur thickness of about 6 nm on the SWCNT surface, the cathode achieved a sulfur content as high as 95%, delivering a specific capacity of 1 280 mAh g^{-1} during the first discharge at a current density of 0.25 A g^{-1}. Additionally, a three-layer composite cathode, prepared by simple stacking, achieved a sulfur loading of 7.2 mg cm^{-2} and an area capacity of 8.6 mAh cm^{-2}. This process exclusively uses sulfur and carbon, eschewing traditional conductive additives and binders, which is advantageous for large-scale production.

However, sulfur-carbon composite cathodes may compromise sulfur utilization at high sulfur loadings. To address this, Yuan et al.[225] devised a hierarchical CNT conductive network structure, combining short MWCNTs with long vertically aligned CNTs to serve as sulfur hosts. This design enabled a CNT-sulfur composite positive electrode to reach an area capacity of 15.1 mAh cm^{-2} at a sulfur area loading of 17.3 mg cm^{-2}, showcasing the high electronic conductivity and the merits of the hierarchical structure.

While individual CNTs offer limited enhancement for LSB performance due to their restricted physical adsorption of LiPSs, further improvements can be attained through stronger chemisorption and chemical bonding. Wu et al.[226] integrated these concepts into LSB cathode host materials, creating an entanglement-free conductive CNT network with highly dispersed Co/N catalytic nodes. This design optimized the electric field distribution and catalyst site homogeneity, achieving an area capacity of 8.86 mAh cm^{-2} at an ultra-high sulfur loading of 13.1 mg cm^{-2} (E/S = 8 μL mg^{-1}). Moreover, it displayed excellent rate performance (473.6 mAh g^{-1} at 20 C) and long-cycle stability (1 200 stable cycles at 1 C), offering innovative directions for LSBs cathode material design with uniform electric field forces and catalytic effects.

Advanced characterization techniques, such as in-situ X-ray diffraction, in-situ Raman spectroscopy, and in-situ TEM, have been increasingly applied to study LSBs. These studies aim to elucidate the reaction mechanisms, thereby enhancing the electrochemical performance of LSBs through various approaches. Despite these efforts, the majority of research has concentrated on the macroscopic sulfur redox process (S_8 to LiPS to Li_2S_2/Li_2S)[227]. There is a recognized gap in the research regarding the detailed reaction principles behind the conversion of carrier materials with Li_2S_2 to Li_2S, a process that is responsible for approximately half of the battery's capacity.

There is a pressing need for a targeted method or mechanism to gain a deeper understanding of the interactions between the substrate materials and sulfur species during the redox process, particularly focusing on the transformation between Li_2S_2 and Li_2S. Additionally, the electron/ion transfer mechanisms at the catalyst interface in LSBs have not been fully unraveled[208]. The phenomenon of partial dead sulfur activation during the oxidation of Li_2S also warrants further investigation[193]. Additionally, theoretical calculations and simulations play a pivotal role in guiding the development of advanced CNT-based Li-S cathode materials. These computational tools offer insights into the structural and chemical properties of potential materials, which can significantly accelerate the discovery and optimization of new materials for LSBs.

3.4 Application of CNTs in sodium batteries

As mentioned above, LIBs have been extensively utilized in electronic products due to their high energy density and good cycle stability. However, the increasing scarcity of lithium resources, a result of continuous mining, poses a challenge. SIBs emerge as a promising energy system for future large-scale EES, leveraging the abundance of sodium reserves and lower development costs[9].

Carbon, the predominant anode material in LIBs, also becomes the go-to material for SIBs due to its plentiful crustal reserves and superior electrical conductivity[228]. Carbon materials, categorized by their dimensions into 0D, 1D, 2D and 3D forms, have been summarized for their physical properties and characteristics by Zhang et al.[229], who also review the progress of carbon-based anodes in Na electrodes. This section focuses on the advancements in CNT-based anode materials for SIBs within the realm of 1D carbon materials.

Zheng et al. uncovered the sodiation/desodiation mechanism of MWCNTs and their mechanical properties through in-situ TEM studies[230]. They observed that the SEI layer tends to grow on the MWCNT surface during sodiation, with Na dendrites resembling fish scales forming as sodiation progresses. An unusual narrowing of the MWCNT width was noted during sodiation, likely due to lattice collapse from Na^+ embedding and the Joule heating effect of MWCNTs. In-situ bending experiments indicated that while pristine MWCNTs possess excellent mechanical properties, sodiated/desodiated MWCNTs are prone to fracture even without external forces. These findings offer valuable insights into MWCNT degradation in SIBs and guide future applications. Zhao et al. created N-doped nanotube structured materials, known as N-CNT, with adjustable interlayer distances through the one-step pyrolysis of *g*-C_3N_4 precursors, aided by a Ni catalyst[231]. They explored the micro-morphological evolution from 2D layer structures to 1D nanotube structures with varying layer spacing (0.342 to 0.462 nm). As an anode for SIBs, N-CNT with a 0.462 nm layer spacing in an ether-based electrolyte demonstrated a remarkable reversible capacity of 290.3 mAh g^{-1} at 0.05 A g^{-1} and 164.5 mAh g^{-1} at 10 A g^{-1}, indicating an ultra-high rate capacity. Over 1 000 cycles, the material showed excellent long-term cycling performance, attributed to its unique 1D structure, high conductivity, and optimal interlayer spacing. Kinetic analysis suggested a significant capacitive storage mechanism of N-CNTs, contributing to its impressive rate capacity and recyclability. Ex-situ Raman and XRD analyses confirmed the insertion/extraction of Na during discharge/charge, with DFT calculations indicating that pyridine N and pyrrole N in the ether-based electrolyte have a stronger Na-adsorption capacity than ester-based electrolytes.

SMBs have garnered attention for their potential in gigawatt-scale energy storage. However, their practical application faces issues such as inefficient cation utilization, dendrite growth, and excessive use of inactive materials[232]. Bai et al. proposed a design for a negative-free Na electrode in SMBs, where various Zn-containing poly-alloys, including ternary and medium/high entropy alloys, were thermally encapsulated by carbon[233]. The interwoven CNTs serve as a lightweight and mechanically flexible substrate for Na deposition, with $NaZn_{13}$ material diffusing uniformly within the CNTs before Na deposition, tuning the Na affinity of the scaffolds without nucleation overpotential. Theoretical and experimental evaluations confirmed preferential Na nucleation within the composite scaffold, directed along the nanotube, achieving up to 10 mAh cm^{-2}.

On the cathode side of SIBs, CNTs primarily function as conductive agents, enhancing the electrochemical performance of Na electricity when combined with active materials. Qin et al. prepared a composite of $Na_3V_2(PO_4)_2F_3$ (NVPF) with a 3D conductive network and CNTs (NVPF/@C/CNTs) using a solvent-heated method[234]. The NVPF nanosheets dispersed into the CNT-formed network, resulting in a discharge specific capacity of 107 mAh g^{-1} after 200 cycles at 0.2 C and 68 mAh g^{-1} at 10 C. The superior electrochemical performance arises from the synergistic combination of nanostructures, carbon coatings, and 3D conductive networks. Yan et al. employed a hydrogel self-templating strategy to produce $Na_3V_2(PO_4)_3$@C@CNT materials with a porous network structure, using 0D nanoparticles and 1D CNTs[235]. The highly conductive CNTs facilitated Na^+ transport during repeated sodiation/desodiation, while the porous structure alleviated volume expansion. The material exhibited excellent cycling stability and rate performance.

The use of CNT materials in SIBs and SMBs capitalizes on their excellent electrical conductivity, combined with various active substances to enhance the material's electrical and chemical properties. Moreover, there is substantial scope for research into flexible Na electrical devices based on CNTs, indicating a promising avenue for future development.

3.5 Application of CNTs in supercapacitors

Supercapacitors are recognized for their rapid power delivery, excellent cycling stability, and safety[236]. These devices typically comprise two electrodes, an electrolyte, and a separator. The charge storage mechanisms of electrode materials, pivotal to the electrochemical performance of supercapacitors, are divided into non-Faraday and Faraday processes[237,238]. In non-Faraday processes, charge storage relies on the electrochemical double-layer capacitance (EDLC), which arises from polarization charge separation at the electrode/electrolyte interface. Carbon materials, owing to their low cost, non-toxicity, chemical stability, high specific surface area, and high electronic conductivity, have become the leading choice for non-Faraday electrode materials[239]. CNTs, in particular, have garnered widespread attention due to their distinctive porous structure, mechanical and thermal stability, and electrical properties[240–242], enabling efficient charge distribution across their accessible surface area through interconnected mesopores.

Li et al. introduced a 3D porous structure composed of micrometer-sized activated carbon (AC), 1D CNT, and 2D reduced graphene oxide (rGO), forming a structured composite material[243]. The CNTs and rGO assembled into a 3D porous framework through van der Waals forces, with the AC being anchored within this structure. The CNTs enhanced the AC's electrical conductivity, while the AC, in turn, prevented CNT aggregation. Collectively, these materials contributed to the overall capacitance, with the AC/CNT/rGO electrode achieving a high specific capacitance of 101 F g^{-1} and a specific energy density of 30 Wh kg^{-1}.

Lee et al. presented an aerogel structure with a layered nanostructure of ternary carbon, comprising graphene oxide, PAN and CNTs (denoted as CNTs@Gr-CNF)[244]. This material offered a highly electroactive surface and excellent electrical conductivity. The CNTs@Gr-CNF electrode demonstrated a high specific capacitance of 521.5 F g^{-1} at 5 A g^{-1}, with a capacitance retention rate of 98% after 10 000 consecutive charge/discharge cycles at 5 A g^{-1}. Furthermore, the team developed a composite supercapacitor device featuring CNTs@Gr-CNF as the negative electrode and $NiCo_2S_4$ nanopins as the positive electrode. This hybrid device delivered a specific capacitance of 218 F g^{-1} at 1 A g^{-1}, a specific energy density of 62.1 Wh kg^{-1}, and a power density of 789.7 W kg^{-1}, along with excellent cycling stability, retaining 91.7% capacitance after 10 000 charge-discharge cycles.

In summary, the application of CNT materials in supercapacitors extends the utility of CNTs in EES devices, with numerous research accomplishments to date. Future developments in CNT-based capacitor devices should concentrate on several key areas[245]. (1) Producing high-purity CNTs and carbon materials with a high specific surface area is essential for achieving high specific capacitance[246]. (2) Enhancing pseudocapacitance can be achieved by introducing abundant surface functional groups and improving electrolyte penetration[247]. (3) Optimizing the electrode fabrication process can reduce internal resistance and enhance rate characteristics, either by directly growing CNTs on a conductive substrate to create an integrated electrode or by manipulating the structure and arrangement of CNTs[248].

3.6 Application of CNTs in flexible EES devices

With the rapid evolution of wearable electronics and portable devices, device concepts such as electronic textiles and flexible smartphones are moving from idea to reality. This shift has created demand for a new generation of batteries characterized by being "lightweight, convenient and flexible"[249]. To better satisfy the needs of modern technology products and the pursuit of a high-quality and eco-friendly lifestyle, there is a pressing need to develop lightweight flexible devices that offer excellent stability[249]. Flexible

energy storage materials have unique requirements compared to their traditional counterparts. They must maintain both electrical and mechanical flexibility, withstand the volume changes associated with the charging and discharging processes of batteries or capacitors, and exhibit resilience to physical deformation[250]. As highlighted earlier, CNTs possess a high Young's modulus, mechanical strength, electrical conductivity, and chemical stability. These attributes make them well-suited for use in flexible electrochemical devices. A significant body of literature already exists, summarizing the applications and research progress of CNTs in flexible devices[27,251,252]. This new section will therefore focus on the latest research developments involving CNTs in flexible EES systems.

Supercapacitors, known for high power density, are an example of EES devices that can benefit from CNT technology. For instance, Zhu et al. fabricated freestanding SWCNT films by FCCVD, employing them as current collectors for flexible supercapacitors[253]. These films are lightweight, highly conductive, mechanically robust, and feature a 3D interconnected porous structure. They support substantial active material loads and demonstrate specific capacitance values of 408.4 F g^{-1} at 1 A g^{-1}, with 90.7% retention after 5 000 cycles, surpassing the performance of conventional current collectors[253]. Moreover, hybrid supercapacitors incorporating materials like cobalt (II) carbonate hydroxide ($Co_2(OH)_2CO_3$) and polyaniline (PANI) have been shown to maintain capacitance stability under various bending conditions[253]. Lu et al. developed CNT@$NiCo_2S_4$ hybrid films, which involve the homogeneous integration of $NiCo_2S_4$ onto 3D CNT networks[254]. This material offers several key benefits for flexible supercapacitors, including an adjustable microstructure, high mechanical flexibility, excellent electrical conductivity, and lightweight design. The resulting supercapacitors exhibit impressive energy densities (59.5/34.5 Wh kg^{-1} at 900/18 000 W kg^{-1}, respectively) and feature a substantial capacity retention of 80.64% after 10 000 cycles. Notably, the material maintains its performance even when bent at angles up to 180°. The performance of these supercapacitors has been successfully demonstrated in wearable devices, underscoring the significant potential of CNTs for use in flexible and wearable EES applications.

The development of flexible batteries requires innovation beyond what is used in traditional batteries. For example, while conventional batteries often use aluminum or copper foils as current collectors, these materials present limitations, particularly in terms of weight and integration with electrode materials[255]. In particular, the high weight of aluminum or copper foils (8−16 mg cm^{-2} of area density) can significantly reduce the overall energy density of a battery. Additionally, the difficulty in establishing strong interactions between these metals and electrode materials can lead to the periodic detachment of active materials from the current collector—a problem that is particularly critical in the flexible battery format. The adoption of CNTs as flexible current collectors has shown promise in overcoming these challenges, as demonstrated by applications in flexible LIBs[256,257]. For instance, Kim et al. employed SWCNTs as current collectors through a direct spinning method for LIBs[256]. This approach resulted in superior rate performance and cycling stability compared to traditional current collectors. The enhanced performance is attributed to 3 key factors: (1) 3D structure of the CNTs, which facilitates effective electrolyte penetration; (2) porous structure, which improves contact with the NCM811 material and provides mechanical adhesion; (3) excellent chemical stability of CNTs in organic electrolytes. The researchers also demonstrated that the assembled pouch cells maintained excellent electrochemical performance even under severe mechanical deformation. Similarly, Hong et al. developed flexible LIBs by integrating nanosilicon with superparabolic CNTs through a structural design that leverages electrostatic interactions[257]. The lightweight CNT interlayer effectively accommodates the volume expansion of silicon during charge and discharge cycles, reducing material loss and enhancing cycling stability. The CNT self-supported electrode exhibited remark-

able flexibility, with resistance changes of only 2.66% and 3.14% after 10 000 cycles at 90° and 180° bending, respectively. Moreover, the flexible pouch cell retained 96% of its capacity after 10 000 cycles at a 90° bending angle, indicating a promising future for commercially viable flexible LIBs.

LSBs, with their higher energy density compared to LIBs, become even more advantageous when integrated with flexible electrodes, potentially reducing the weight and volume of wearable devices[258]. Research results indicate that the development of flexible LSBs must account for the flexibility of the entire battery assembly, including the lithium metal anode, separator, and sulfur cathode, while also addressing the challenges inherent in conventional LSBs[259,260]. Chen et al. have highlighted that employing soft structures and soft materials are 2 critical strategies for constructing flexible batteries[258]. However, relying solely on one strategy may limit the improvements achieved. Building on the previous sections that discussed the use of CNTs as an intermediate layer in self-supporting separators for LSBs, we will now turn to the application of flexible electrodes in LSB cathodes. Liu et al. utilized lignin as a carbon source to fabricate flexible CNT films through the FCCVD technique[261]. These films demonstrated impressive mechanical strength of 54.53 MPa and electrical conductivity of 4.19×10^4 S m^{-1}. When integrated into an LSB cathode and assembled into a battery, they sustained capacities of 706.1 mAh g^{-1} at 0.5 C and 435.3 mAh g^{-1} at 2.0 C for 200 cycles, respectively. Moreover, a lithium-sulfur flexible pouch cell with a CNT film cathode was capable of powering a small light bulb even when subjected to bending from 0° to 180°, showcasing its practical applicability in flexible electronics.

The integration of CNTs with other materials, such as graphene, demonstrates their versatility and potential to enhance performance in flexible EES devices. Such composites prevent agglomeration and establish a 3D conductive network, which is crucial for device performance[262]. Despite significant strides, the development of flexible EES devices is still in a relatively early stage and many challenges remain[27,255]. The advancement of high-performance CNT components, including fibers, films and aerogels, is essential. These components require further investigation to achieve stronger mechanical properties, lighter and thinner materials, and more scalable and convenient preparation processes. Additionally, controllable functionalization of CNTs is necessary to balance electrical conductivity, mechanical properties, chemical stability, energy density, and power density. Another challenge is the development of flexible solid or gel electrolytes that are compatible with flexible devices. These electrolytes must prevent leakage during the mechanical stress associated with repeated bending, stretching, and compression. Moreover, improving the performance evaluation criteria is vital. Unlike traditional batteries, flexible batteries require criteria that account for tensile or bending mechanical deformation, electrochemical performance under dynamic conditions, and overall energy and power densities. While CNT materials have been successfully utilized in a variety of flexible EES devices due to their excellent mechanical stability, there is a need for ongoing research to refine these materials and address the aforementioned challenges. Future work must focus on enhancing the mechanical properties of CNT components and developing performance evaluation criteria that reflect the unique dynamic conditions of flexible devices.

4 Summary and outlook

The exploration of CNTs in the realm of EES has unveiled their multifaceted potential, underlining their significance in advancing sustainable energy technologies. Over the past decades, the synthesis of CNTs has evolved significantly, focusing on two major trends: (1) Controlling the fine structure, including tube diameter, electronic structure, and chirality and trends; (2) Controlling the macroscopic structure, including large-scale production technology and the design of CNT aggregate materials[53]. This review has comprehensively examined the properties, synthesis, and EES applications of CNTs, highlighting their ex-

ceptional mechanical strength, electrical conductivity, and thermal performance. The comparison with other carbon materials has further emphasized CNTs' superior electrical conductivity, a trait that is invaluable for EES applications.

The synthesis methods discussed, including AD, LA, and CVD, have shed light on the industrial relevance and challenges of large-scale production. Among these, CVD technology shows great potential for the development of fine structure-controlled synthesis of CNTs due to its excellent stability and diverse design space. The tube diameter of CNTs can be tuned mainly by conditions such as the size of the catalyst, the type and partial pressure of the carbon source, and the reaction temperature[263]. However, achieving a uniform distribution of catalyst particle sizes remains a challenge, affecting the control over individual CNT diameters. The advent of novel synthesis techniques, such as those utilizing MOFs and template-assisted methods demonstrate the capability to produce CNTs with orderly porous structures. Our group's investigation into a straightforward calcination approach for synthesizing CNTs with 3DOM structures at lower temperatures exemplifies the continuous innovation within this domain.

The application of CNTs in various EES devices, such as LIBs, LSBs, LMBs, SIBs and supercapacitors, has demonstrated their widespread utility. However, the field is not without its challenges. The traditional slurry coating method for electrode fabrication, for instance, introduces inactive binders that reduce the overall energy density of the battery system. The development of integrated monolithic electrodes, which minimize the use of inactive materials, represents a promising direction for future EES advancements[264].

In terms of fine structure control, the preparation of CNTs with specific structures is essential[265]. The relationship between the diameter of CNTs and the catalyst size is crucial, as it is closely related to the growth mechanism of CNTs[263]. A synergistic method involving electrochemical truncation and selective adsorption has been designed to control the preparation of CNTs, efficiently regulating their lengths and length distributions[266]. The preparation of CNTs with specific electronic structures is even more critical. Only SWCNTs with homogeneous properties (metallic/semiconducting) tend to fulfill the corresponding requirements in most electronic applications. Liquid phase separation, post-processing, and direct growth are the main methods for separating CNTs with different electronic properties. The direct growth method is relatively the most advantageous and has been reported in the literature[267]. However, achieving selectivity of CNTs with a single property over 99% is still difficult due to the small differences between the two CNT growth processes.

The synthesis of chiral controllable CNTs (for SWCNT only) is another area of focus. Many properties of CNTs depend on their topology (i.e., chirality). The control of CNT chirality is mainly focused on the end-cap or seed structure, aiming to synthesize a specific chirality at an early stage. CVD technology is expected to play an extremely important role in this regard, and the thermodynamic and kinetic modulation of CNT structure based on catalytic growth will surely play an important role in the future.

Furthermore, the synthesis of CNT aggregates is vital for fully utilizing the advantages of individual CNTs. The properties of CNT aggregate materials are often greatly reduced due to internal impurities, defects, entanglement, and other factors. Therefore, developing CNT aggregate materials with excellent electrical, mechanical, and thermal conductivity properties is especially important for the application of EES systems.

In conclusion, the future of CNTs in EES is bright but requires a concerted effort to overcome existing challenges. Interdisciplinary collaboration will be key in this endeavor, bringing together expertise from materials science, electrical engineering, nanotechnology, and environmental science. By harnessing a multidisciplinary approach, researchers can design and optimize CNT-based materials for enhanced performance, improved safety, and reduced environmental impact.

The path forward should focus on several stra-

tegic areas. First, there is a need to refine the synthesis processes to improve the uniformity and purity of CNTs, particularly for industrial-scale applications. Second, the development of environmentally friendly and low-cost process technologies for the high-volume synthesis and fabrication of CNT-based nanocomposites is essential. Third, safety assessments of CNTs in EES systems are essential, addressing mechanical stability[268], electrochemical reliability[269], and health and environmental effects[270]. A balanced approach, prioritizing both the advantages and proactive risk mitigation of CNTs, is crucial for developing secure and efficient EES solutions. Lastly, the integration of theoretical calculations, simulations, and advanced characterization techniques will be pivotal strategies in guiding the development of advanced CNT-based materials. As we look to the horizon, the continued research and innovation in the field of CNTs hold the promise of transforming the landscape of EES technologies, moving us closer to a sustainable and energy-secure future.

Declarations

The authors declare no interest conflict. They have no known competing financial interests or personal relationships that could have appeared to influence the work reported in this paper.

Acknowledgements

This work was sponsored by National Natural Science Foundation of China (22379110) and Natural Science Foundation of Tianjin (20JCQNJC01280).

References

[1] Liu Y, Yu Z, Chen J, et al. Recent development and progress of structural energy devices[J]. Chinese Chemical Letters, 2022, 33(4): 1817-1830.

[2] Zhai Y, Dou Y, Zhao D, et al. Carbon materials for chemical capacitive energy storage[J]. Advanced Materials, 2011, 23(42): 4828-4850.

[3] Li M, Lu J, Chen Z, et al. 30 years of lithium-ion batteries[J]. Advanced Materials, 2018, 30(33): 1800561.

[4] Gur T M. Review of electrical energy storage technologies, materials and systems: Challenges and prospects for large-scale grid storage[J]. Energy & Environmental Science, 2018, 11(10): 2696-2767.

[5] Choi J W, Aurbach D. Promise and reality of post-lithium-ion batteries with high energy densities[J]. Nature Reviews Materials, 2016, 1(4): 1-16.

[6] Lyu T, Luo F, Wang D, et al. Carbon/lithium composite anode for advanced lithium metal batteries: Design, progress, in situ characterization, and perspectives[J]. Advanced Energy Materials, 2022, 12(36): 2201493.

[7] Deng R, Wang M, Yu H, et al. Recent advances and applications toward emerging lithium-sulfur batteries: Working principles and opportunities[J]. Energy & Environmental Materials, 2022, 5(3): 777-799.

[8] Zhou G, Chen H, Cui Y. Formulating energy density for designing practical lithium-sulfur batteries[J]. Nature Energy, 2022, 7(4): 312-319.

[9] Hwang J Y, Myung S T, Sun Y K. Sodium-ion batteries: Present and future[J]. Chemical Society Reviews, 2017, 46(12): 3529-3614.

[10] Najib S, Erdem E. Current progress achieved in novel materials for supercapacitor electrodes: mini review[J]. Nanoscale Advances, 2019, 1(8): 2817-2827.

[11] Ajayan P M. The nano-revolution spawned by carbon[J]. Nature, 2019, 575(7781): 49-50.

[12] Geng C, Chen Y X, Shi L L, et al. Design of active sites in carbon materials for electro-chemical potassium storage[J]. New Carbon Materials, 2022, 37(3): 461-483.

[13] Rathinavel S, Priyadharshini K, Panda D. A review on carbon nanotube: An overview of synthesis, properties, functionalization, characterization, and the application[J]. Materials Science and Engineering B-Advanced Functional Solid-State Materials, 2021, 268: 115095.

[14] Chen Y, Xi B, Huang M, et al. Defect-selectivity and "order-in-disorder" engineering in carbon for durable and fast potassium storage[J]. Advanced Materials, 2022, 34(7): 2108621.

[15] Sun Z, Chen Y, Xi B, et al. Edge-oxidation-induced densification towards hybrid bulk carbon for low-voltage, reversible and fast potassium storage[J]. Energy Storage Materials, 2022, 53: 482-491.

[16] De Volder M F L, Tawfick S H, Baughman R H, et al. Carbon nanotubes: Present and future commercial applications[J]. Science, 2013, 339(6119): 535-539.

[17] Rodriguez N M. A review of catalytically grown carbon nanofibers[J]. Journal of Materials Research, 1993, 8(12): 3233-3250.

[18] Lijima S. Helical microtubules of graphitic carbon[J]. Nature, 1991, 354: 56-58.

[19] Qiu L, Ding F. Understanding single-walled carbon nanotube growth for chirality controllable synthesis[J]. Accounts of Materials Research, 2021, 2(9): 828-841.

[20] Chiang W H, Sankaran R M. Linking catalyst composition to chirality distributions of as-grown single-walled carbon nanotubes

by tuning Ni_xFe_{1-x} nanoparticles[J]. Nature Materials, 2009, 8(11): 882-886.

[21] Dresselhaus M S, Dresselhaus G, Saito R, et al. Raman spectroscopy of carbon nanotubes[J]. Physics Reports, 2005, 409(2): 47-99.

[22] Dillon A C. Carbon nanotubes for photoconversion and electrical energy storage[J]. Chemical Reviews, 2010, 110(11): 6856-6872.

[23] Chew S Y, Ng S H, Wang J, et al. Flexible free-standing carbon nanotube films for model lithium-ion batteries[J]. Carbon, 2009, 47(13): 2976-2983.

[24] Zhou X, Zhou J J, Ou-Yang Z C. Strain energy and Young's modulus of single-wall carbon nanotubes calculated from electronic energy-band theory[J]. Physical Review B, 2000, 62(20): 13692-13696.

[25] Peng B, Locascio M, Zapol P, et al. Measurements of near-ultimate strength for multiwalled carbon nanotubes and irradiation-induced crosslinking improvements[J]. Nature Nanotechnology, 2008, 3(10): 626-631.

[26] Treacy M M J, Ebbesen T W, Gibson J M. Exceptionally high Young's modulus observed for individual carbon nanotubes[J]. Nature, 1996, 381: 678-680.

[27] Wen L, Li F, Cheng H M. Carbon nanotubes and graphene for flexible electrochemical energy storage: From materials to devices[J]. Advanced Materials, 2016, 28(22): 4306-4337.

[28] Kim H, Cheong J Y, Hwang B. Mini review of technological trends of flexible supercapacitors using carbon nanotubes[J]. Journal of Natural Fibers, 2023, 20(2): 2204455.

[29] Wang L, Wen R L, Deng J G, et al. A first-principles study of B/N doping on the transport properties of ultrafine single-walled carbon nanotubes[J]. Chinese Journal of Physics, 2023, 85: 571-582.

[30] White C T, Todorov T N. Carbon nanotubes as long ballistic conductors[J]. Nature, 1998, 393(6682): 240-242.

[31] Yao Z, Kane C L, Dekker C. High-field electrical transport in single-wall carbon nanotubes[J]. Physical Review Letters, 2000, 84(13): 2941-2944.

[32] Ma P-C, Siddiqui N A, Marom G, et al. Dispersion and functionalization of carbon nanotubes for polymer-based nanocomposites: A review[J]. Composites Part A-Applied Science and Manufacturing, 2010, 41(10): 1345-1367.

[33] Zhang B A, Kang F Y, Tarascon J M, et al. Recent advances in electrospun carbon nanofibers and their application in electrochemical energy storage[J]. Progress in Materials Science, 2016, 76: 319-380.

[34] Sun Y, Shi X L, Yang Y L, et al. Biomass-derived carbon for high-performance batteries: From structure to properties[J]. Advanced Functional Materials, 2022, 32(24): 2201584.

[35] Zhong M, Zhang M, Li X. Carbon nanomaterials and their composites for supercapacitors[J]. Carbon Energy, 2022, 4(5): 950-985.

[36] Javey A, Guo J, Wang Q, et al. Ballistic carbon nanotube field-effect transistors[J]. Nature, 2003, 424(6949): 654-657.

[37] Xiao L, Chen Z, Feng C, et al. Flexible, stretchable, transparent carbon nanotube thin film loudspeakers[J]. Nano Letters, 2008, 8(12): 4539-4545.

[38] Yadav D, Sanserwal M. A comprehensive review of the effects of various factors on the thermal conductivity and rheological characteristics of CNT nanofluids[J]. Journal of Thermal Analysis and Calorimetry, 2023, 148(5): 1723-1763.

[39] Wang R, Wang R, Wang Y. Ex-situ measurement of thermal conductivity and swelling of nanostructured fibrous electrodes in electrochemical energy devices[J]. Thermal Science and Engineering Progress, 2021, 21: 100805.

[40] Han S E, Go H, Lee H, et al. Enhanced field emission properties of CNT film emitters through densification using nitric acid[J]. ACS Applied Electronic Materials, 2024, 6(3): 2039-2048.

[41] Xing Z, Hao X, Su W, et al. Infrared emission enhancement of a black coating doped with multiwall carbon nanotubes using multi-spraying method[C]. AOPC 2021: Infrared Device and Infrared Technology, 2021.

[42] Liu S, Cui N, Wu Q, et al. Laser switching characteristics of enriched (7, 5) single-walled carbon nanotubes at 640 nm[J]. Carbon, 2022, 191: 433-438.

[43] Utsumi S, Ujjain S K, Takahashi S, et al. Giant nanomechanical energy storage capacity in twisted single-walled carbon nanotube ropes[J]. Nature nanotechnology, 2024.

[44] Castellanos-Leal E, Martínez-Guerra E, Chavez-Valdez A, et al. Effect of the reinforcement phase on the electrical and mechanical properties of Cu-SWCNTs nanocomposites[J]. Diamond and Related Materials, 2024, 142: 110765.

[45] Mercadal J J, Mayoral A, Fierrod J L G, et al. Improved O_2-assisted styrene synthesis by double-function purification of SWCNT catalyst[J]. Chemical Engineering Journal, 2023, 455: 140723.

[46] Pandit B, Rondiya S R, Cross R W, et al. Vanadium telluride nanoparticles on MWCNTs prepared by successive ionic layer adsorption and reaction for solid-state supercapacitor[J]. Chemical Engineering Journal, 2022, 429: 132505.

[47] Fan W, Zhao J, Liu D, et al. Synthesis of Mo_2C@MWCNTs and its application in improving the electrochemical hydrogen storage properties of $Co_{0.9}Cu_{0.1}Si$ alloy[J]. Journal of Energy Storage, 2023, 72(15): 108264.

[48] Wang M, Qin Y, Gao W, et al. Lightweight MWCNT/hollow mesoporous carbon/WPU composite material with excellent electromagnetic shielding performance[J]. RSC Advances, 2021, 11(59): 37194-37204.

[49] Feng Z, He Q, Wang X, et al. Capacitive sensors with hybrid dielectric structures and high sensitivity over a wide pressure range for monitoring biosignals[J]. ACS Applied Materials & Interfaces, 2023, 15(4): 6217-6227.

[50] Lu P, Wang X, Wen L, et al. Silica-mediated formation of nickel sulfide nanosheets on CNT films for versatile energy storage[J]. Small, 2019, 15(15): 1805064.

[51] Hakim M W, Ali I, Fatima S, et al. Enhanced electrochemical performance of MWCNT-assisted molybdenum-titanium carbide MXene as a potential electrode material for energy storage application[J]. ACS Omega, 2024, 9(8): 8763-8772.

[52] Wei X, Li S, Wang W, et al. Recent advances in structure separation of single-wall carbon nanotubes and their application in optics, electronics, and optoelectronics[J]. Advanced Science, 2022, 9(14): 2200054.

[53] 张锦, 张莹莹. 碳纳米管的结构控制生长[M]. 北京: 科学出版社, 2019.
(Zhang J, Zhang Y. Carbon Nanotubes: Growth Mechanism and Structure Control[M]. Beijing: Science Press, 2019.)

[54] Lin Y M, Appenzeller J, Chen Z H, et al. High-performance dual-gate carbon nanotube FETs with 40-nm gate length[J]. IEEE Electron Device Letters, 2005, 26(11): 823-825.

[55] Wang X, Dong A, Hu Y, et al. A review of recent work on using metal-organic frameworks to grow carbon nanotubes[J]. Chemical Communications, 2020, 56(74): 10809-10823.

[56] Ahmad M, Silva S R P. Low temperature growth of carbon nanotubes: A review[J]. Carbon, 2020, 158: 24-44.

[57] 王疆. 有序大孔类石墨烯碳质复合材料的创制及储能性能研究[D]. 天津: 天津大学, 2022.
(Wang J. Development and electrochemical energy storage performance of ordered macroporous graphene-like carbon composite materials[D]. Tianjin: Tianjin University, 2022.)

[58] Zhang Q, Huang J Q, Zhao M Q, et al. Carbon nanotube mass production: Principles and processes[J]. ChemSusChem, 2011, 4(7): 864-889.

[59] Islam M H, Afroj S, Uddin M A, et al. Graphene and CNT-based smart fiber-reinforced composites: A Review[J]. Advanced Functional Materials, 2022, 32(40): 2205723.

[60] Kamyshny A, Magdassi S. Conductive nanomaterials for 2D and 3D printed flexible electronics[J]. Chemical Society Reviews, 2019, 48(6): 1712-1740.

[61] Truus K, Volobujeva O, Kaupmees R, et al. Recent advances of carbon nanotubes synthesis by the electric arc technique using atomized platinum-group metal catalysts[J]. Materials Science and Engineering B-Advanced Functional Solid-State Materials, 2024, 300: 117121.

[62] Li H J, Guan L H, Shi Z J, et al. Direct synthesis of high purity single-walled carbon nanotube fibers by arc discharge[J]. Journal of Physical Chemistry B, 2004, 108(15): 4573-4575.

[63] Arora N, Sharma N N. Effect of current variation on carbon black to synthesize MWCNTs using pulsed arc discharge method[C]. International Conference on Recent Trends in Engineering and Material Sciences (ICEMS), 2016: 9394-9398.

[64] Shifa M, Toor Z S, Tariq F. Arc discharge synthesis and multistep purification of multiwall carbon nanotubes[J]. Nano, 2024, 19(02): 2450007.

[65] Wang Z, Zhao Z, Qiu J. In situ synthesis of super-long Cu nanowires inside carbon nanotubes with coal as carbon source[J]. Carbon, 2006, 44(9): 1845-1847.

[66] Roch A, Jost O, Schultrich B, et al. High-yield synthesis of single-walled carbon nanotubes with a pulsed arc-discharge technique[J]. Physica Status Solidi B-Basic Solid State Physics, 2007, 244(11): 3907-3910.

[67] Zhao S, Hong R, Luo Z, et al. Carbon nanostructures production by ac arc discharge plasma process at atmospheric pressure[J]. Journal of Nanomaterials, 2011, 2011: 346206.

[68] Maria K H, Mieno T. Synthesis of single-walled carbon nanotubes by low-frequency bipolar pulsed arc discharge method[J]. Vacuum, 2015, 113: 11-18.

[69] Zhang Y L, Hou P X, Liu C, et al. De-bundling of single-wall carbon nanotubes induced by an electric field duringarc discharge synthesis[J]. Carbon, 2014, 74: 370-373.

[70] Sharma R, Sharma A K, Sharma V, et al. Synthesis of carbon nanotubes by arc-discharge and chemical vapor deposition method with analysis of its morphology, dispersion and functionalization characteristics[J]. Cogent Engineering, 2015, 2(1): 1094017.

[71] Sari A. H, Khazali A, Parhizgar S S. Synthesis and characterization of long-CNTs by electrical arc discharge in deionized water and NaCl solution[J]. International Nano Letters, 2018, 8(1): 19-23.

[72] Roslan M S, Chaudhary K T, Doylend N, et al. Growth of wall-controlled MWCNTs by magnetic field assisted arc discharge plasma[J]. Journal of Saudi Chemical Society, 2019, 23(2): 171-181.

[73] Guo T, Nikolaev P, Rinzler A W, et al. Self assembly of tubular fullerenes[J]. Journal of Physical Chemistry, 1995, 99(27): 10694-10697.

[74] Braidy N, El Khakani M A, Botton G A. Effect of laser intensity on yield and physical characteristics of single wall carbon nanotubes produced by the Nd: YAG laser vaporization method[J]. Carbon, 2002, 40(15): 2835-2842.

[75] Maser W, Muñoz E, Benito A, et al. Production of high-density single-walled nanotube material by a simple laser-ablation method[J]. Chemical Physics Letters, 1998, 292(4-6): 587-593.

[76] Chen S, Chen Y, Xu H, et al. Single-walled carbon nanotubes synthesized by laser ablation from coal for field-effect transistors[J]. Materials Horizons, 2023, 10(11): 5185-5191.

[77] Ruan W, Wang Z, Li J, et al. Synthesis of carbon nanotubes on suspending microstructures by rapid local laser heating[J]. IEEE Sensors Journal, 2011, 11(12): 3424-3425.

[78] Uchida T, Yoshida Y. Development of a laser-assisted chemical vapor deposition system for the growth of carbon nanotubes[J]. Journal of Laser Micro Nanoengineering, 2011, 6(3): 214-219.

[79] Bock M C D, Denk R, Wirth C T, et al. Optical feedback mechanisms in laser induced growth of carbon nanotube forests[J]. Applied Physics Letters, 2012, 100(1): 013112.

[80] Kumar M, Ando Y. Chemical vapor deposition of carbon nanotubes: A review on growth mechanism and mass production[J]. Journal of Nanoscience and Nanotechnology, 2010, 10(6): 3739-3758.

[81] Shah K A, Tali B A. Synthesis of carbon nanotubes by catalytic

chemical vapour deposition: A review on carbon sources, catalysts and substrates[J]. Materials Science in Semiconductor Processing, 2016, 41: 67-82.

[82] Pant M, Singh R, Negi P, et al. A comprehensive review on carbon nano-tube synthesis using chemical vapor deposition[C]. International Conference on Technological Advancements in Materials Science and Manufacturing (ICTAMSM), 2021: 11250-11253.

[83] Yang Y, Zhang H, Yan Y. Synthesis of CNTs on stainless steel microfibrous composite by CVD: Effect of synthesis condition on carbon nanotube growth and structure[J]. Composites Part B-Engineering, 2019, 160: 369-383.

[84] Huynh T M, Nguyen S, Nguyen N T K, et al. Effects of catalyst pretreatment on carbon nanotube synthesis from methane using thin stainless-steel foil as catalyst by chemical vapor deposition method[J]. Nanomaterials, 2021, 11(1): 50.

[85] Thapa A, Neupane S, Guo R, et al. Direct growth of vertically aligned carbon nanotubes on stainless steel by plasma enhanced chemical vapor deposition[J]. Diamond and Related Materials, 2018, 90: 144-153.

[86] Mckee G S B, Deck C P, Vecchio K S. Dimensional control of multi-walled carbon nanotubes in floating-catalyst CVD synthesis[J]. Carbon, 2009, 47(8): 2085-2094.

[87] Mubarak N M, Yusof F, Alkhatib M F. The production of carbon nanotubes using two-stage chemical vapor deposition and their potential use in protein purification[J]. Chemical Engineering Journal, 2011, 168(1): 461-469.

[88] Li Y, Zhang X B, Tao X Y, et al. Single phase $MgMoO_4$ as catalyst for the synthesis of bundled multi-wall carbon nanotubes by CVD[J]. Carbon, 2005, 43(6): 1325-1328.

[89] Ruemmeli M H, Schaeffel F, Bachmatiuk A, et al. Investigating the the outskirts of Fe and Co catalyst particles in alumina-supported catalytic CVD carbon nanotube growth[J]. ACS Nano, 2010, 4(2): 1146-1152.

[90] Shirazi Y, Tofighy M A, Mohammadi T, et al. Effects of different carbon precursors on synthesis of multiwall carbon nanotubes: Purification and functionalization[J]. Applied Surface Science, 2011, 257(16): 7359-7367.

[91] Hata K, Futaba D N, Mizuno K, et al. Water-assisted highly efficient synthesis of impurity-free single-walled carbon nanotubes[J]. Science, 2004, 306(5700): 1362-1364.

[92] Li D, Tong L, Gao B. Synthesis of multiwalled carbon nanotubes on stainless steel by atmospheric pressure microwave plasma chemical vapor deposition[J]. Applied Sciences-Basel, 2020, 10(13): 4468.

[93] Qiu J S, An Y L, Zhao Z B, et al. Catalytic synthesis of single-walled carbon nanotubes from coal gas by chemical vapor deposition method[J]. Fuel Processing Technology, 2004, 85(8-10): 913-920.

[94] Baker R T K, Harris P S, Thomas B, et al. Formation of filamentous carbon from iron, cobalt and chromium catalyzed decomposition of acetylene[J]. Journal of Catalysis, 1973, 30: 86-95.

[95] Hofmann S, Blume R, Wirth C T, et al. State of transition metal catalysts during carbon nanotube growth[J]. Journal of Physical Chemistry C, 2009, 113(5): 1648-1656.

[96] Downs W. B, Baker R T K. Novel carbon fiber-carbon filament structures[J]. Carbon, 1991, 29(8): 1173-1179.

[97] Melechko A V, Merkulov V I, Mcknight T E, et al. Vertically aligned carbon nanofibers and related structures: Controlled synthesis and directed assembly[J]. Journal of Applied Physics, 2005, 97(4): 041301.

[98] Zhang R, Zhang Y, Zhang Q, et al. Growth of half-meter long carbon nanotubes based on Schulz-Flory distribution[J]. ACS Nano, 2013, 7(7): 6156-6161.

[99] Zhu Z, Wei N, Cheng W, et al. Rate-selected growth of ultrapure semiconducting carbon nanotube arrays[J]. Nature Communications, 2019, 10: 4467.

[100] Fan S S, Chapline M G, Franklin N R, et al. Self-oriented regular arrays of carbon nanotubes and their field emission properties[J]. Science, 1999, 283(5401): 512-514.

[101] Gautier L-A, Le Borgne V, El Khakani M A. Field emission properties of graphenated multi-wall carbon nanotubes grown by plasma enhanced chemical vapour deposition[J]. Carbon, 2016, 98: 259-266.

[102] Meyyappan M. A review of plasma enhanced chemical vapour deposition of carbon nanotubes[J]. Journal of Physics D-Applied Physics, 2009, 42(21): 213001-213015.

[103] Sato H, Sakai T, Suzuki A, et al. Growth control of carbon nanotubes by plasma enhanced chemical vapor deposition[J]. Vacuum, 2008, 83(3): 515-517.

[104] Popov V N. Carbon nanotubes: properties and application[J]. Materials Science & Engineering R-Reports, 2004, 43(3): 61-102.

[105] Gupta N, Gupta S M, Sharma S K. Carbon nanotubes: Synthesis, properties and engineering applications[J]. Carbon Letters, 2019, 29(5): 419-447.

[106] Su P, Xiao H, Zhao J, et al. Nitrogen-doped carbon nanotubes derived from Zn-Fe-ZIF nanospheres and their application as efficient oxygen reduction electrocatalysts with in situ generated iron species[J]. Chemical Science, 2013, 4(7): 2941-2946.

[107] Li Q, Wu J, Huang L, et al. Sulfur dioxide gas-sensitive materials based on zeolitic imidazolate framework-derived carbon nanotubes[J]. Journal of Materials Chemistry A, 2018, 6(25): 12115-12124.

[108] Xia B Y, Yan Y, Li N, et al. A metal-organic framework-derived bifunctional oxygen electrocatalyst[J]. Nature Energy, 2016, 1: 1-8.

[109] Wang S, Qin J, Meng T, et al. Metal-organic framework-induced construction of actiniae-like carbon nanotube assembly as advanced multifunctional electrocatalysts for overall water splitting and Zn-air batteries[J]. Nano Energy, 2017, 39: 626-638.

[110] Liu L, Wang Y, Yan F, et al. Cobalt-encapsulated nitrogen-doped carbon nanotube arrays for flexible zinc-air batteries[J]. Small Methods, 2020, 4(1): 1900571.

[111] 吉科猛, 王疆, 刘召召, 等. 一种碳纳米管构成的三维有序大孔炭材料及其制备方法[P]. 国家授权发明专利, 专利号: ZL202110658668.5.
(Ji K, Wang J, Liu Z, et al. Carbon nanotube (CNT)-based three-dimensional ordered macroporous (3DOM) carbon material and preparation method thereof[P]. National authorized invention patent, No. : ZL202110658668.5.)

[112] Ji K, Liang G, Shen Y, et al. Ordered macroporous graphenic carbon-based framework materials and their low-temperature co-sacrificial template synthesis mechanism[J]. Cell Reports Physical Science, 2023, 4(2): 101283.

[113] Ribeiro H, Schnitzler M C, Da Silva W M, et al. Purification of carbon nanotubes produced by the electric arc-discharge method[J]. Surfaces and Interfaces, 2021, 26: 101389.

[114] Huang L, Wu B, Chen J, et al. Synthesis of single-walled carbon nanotubes by an arc-discharge method using selenium as a promoter[J]. Carbon, 2011, 49(14): 4792-4800.

[115] Wu L, Liu J, Reddy B R, et al. Preparation of coal-based carbon nanotubes using catalytical pyrolysis: A brief review[J]. Fuel Processing Technology, 2022, 229: 107171.

[116] Ruan C, Chen M. Hierarchical carbon nanotube/nanocapsule composite via a facile arc discharge approach for high-frequency microwave absorption[J]. Materials Letters, 2019, 249: 87-90.

[117] Su Y, Zhang Y. Carbon nanomaterials synthesized by arc discharge hot plasma[J]. Carbon, 2015, 83: 90-99.

[118] Ismail R A, Mohsin M H, Ali A K, et al. Preparation and characterization of carbon nanotubes by pulsed laser ablation in water for optoelectronic application[J]. Physica E-Low-Dimensional Systems & Nanostructures, 2020, 119: 113997.

[119] Kang S, Han H, Mhin S, et al. Ni-doped carbon nanotubes fabricated by pulsed laser ablation in liquid as efficient electrocatalysts for oxygen evolution reaction[J]. Applied Surface Science, 2021, 547: 149197.

[120] Mehrabi M, Reyhani A, Parvin P, et al. Surface structural alteration of multi-walled carbon nanotubes decorated by nickel nanoparticles based on laser ablation/chemical reduction methods to enhance hydrogen storage properties[J]. International Journal of Hydrogen Energy, 2019, 44(7): 3812-3823.

[121] Hou P X, Zhang F, Zhang L, et al. Synthesis of carbon nanotubes by floating catalyst chemical vapor deposition and their applications[J]. Advanced Functional Materials, 2022, 32(11): 2108541.

[122] Manawi Y M, Ihsanullah, Samara A, et al. Review of carbon nanomaterials' synthesis via the chemical vapor deposition (CVD) method[J]. Materials, 2018, 11(5): 822.

[123] Zhang Q, Wei N, Laiho P, et al. Recent developments in single-walled carbon nanotube thin films fabricated by dry floating catalyst chemical vapor deposition[J]. Topics in Current Chemistry, 2017, 375(6): 90.

[124] Firouzi A, Sobri S, Yasin F M, et al. Synthesis of carbon nanotubes by chemical vapor deposition and their application for CO_2 and CH_4 detection[C]. International Conference on Nanotechnology and Biosensors, 2010.

[125] Dong L, Park J G, Leonhardt B E, et al. Continuous synthesis of double-walled carbon nanotubes with water-assisted floating catalyst chemical vapor deposition[J]. Nanomaterials, 2020, 10(2): 365.

[126] Ji H, Wang J, Ma J, et al. Fundamentals, status and challenges of direct recycling technologies for lithium ion batteries[J]. Chemical Society Reviews, 2023, 52: 8194-8244.

[127] Oh P, Yun J, Park S, et al. Recent advances and prospects of atomic substitution on layered positive materials for lithium-ion battery[J]. Advanced Energy Materials, 2021, 11(15): 2003197.

[128] Zheng Y, Yao Y, Ou J, et al. A review of composite solid-state electrolytes for lithium batteries: Fundamentals, key materials and advanced structures[J]. Chemical Society Reviews, 2020, 49(23): 8790-8839.

[129] Yuan S, Lai Q H, Duan X, et al. Carbon-based materials as anode materials for lithium-ion batteries and lithium-ion capacitors: A review[J]. Journal of Energy Storage, 2023, 61: 106716.

[130] Jin Y, Zhu B, Lu Z, et al. Challenges and recent progress in the development of Si anodes for lithium-ion battery[J]. Advanced Energy Materials, 2017, 7(23): 1700715.

[131] Wu J, Qin X, Miao C, et al. A honeycomb-cobweb inspired hierarchical core-shell structure design for electrospun silicon/carbon fibers as lithium-ion battery anodes[J]. Carbon, 2016, 98: 582-591.

[132] Yan Y, Li C, Liu C, et al. Bundled and dispersed carbon nanotube assemblies on graphite superstructures as free-standing lithium-ion battery anodes[J]. Carbon, 2019, 142: 238-244.

[133] Mcbrayer J D, Rodrigues M-T F, Schulze M C, et al. Calendar aging of silicon-containing batteries[J]. Nature Energy, 2021, 6(9): 866-872.

[134] Cao C, Abate I I, Sivonxay E, et al. Solid electrolyte interphase on native oxide-terminated silicon anodes for Li-Ion batteries[J]. Joule, 2019, 3(3): 762-781.

[135] Guo X, Sun B, Su D, et al. Recent developments of aprotic lithium-oxygen batteries: Functional materials determine the electrochemical performance[J]. Science Bulletin, 2017, 62(6): 442-452.

[136] Luo W, Chen X, Xia Y, et al. Surface and interface engineering of silicon-based anode materials for lithium-ion batteries[J]. Advanced Energy Materials, 2017, 7(24): 1701083.

[137] Shimizu M, Usui H, Matsumoto K, et al. Effect of cation structure of ionic liquids on anode properties of Si electrodes for LIB[J]. Journal of the Electrochemical Society, 2014, 161(12): A1765-A1771.

[138] Feng K, Li M, Liu W, et al. Silicon-based anodes for lithium-ion batteries: From fundamentals to practical applications[J]. Small, 2018, 14(8): 1702737.

[139] Zhang Y, Du N, Yang D. Designing superior solid electrolyte interfaces on silicon anodes for high-performance lithium-ion batteries[J]. Nanoscale, 2019, 11(41): 19086-19104.

[140] Xia C, Kwok C Y, Nazar L F. A high-energy-density lithium-

oxygen battery based on a reversible four-electron conversion to lithium oxide[J]. Science, 2018, 361(6404): 777-781.

[141] Nzabahimana J, Guo S, Hu X. Facile synthesis of Si@void@C nanocomposites from low-cost microsized Si as anode materials for lithium-ion batteries[J]. Applied Surface Science, 2019, 479: 287-295.

[142] Pan S, Han J, Wang Y, et al. Integrating SEI into layered conductive polymer coatings for ultrastable silicon anodes[J]. Advanced Materials, 2022, 34(31): 2203617.

[143] Zhang Z Y, Li Z W, Luo Q, et al. Spontaneous nanominiaturization of silicon microparticles with structural stability as flexible anodes for lithium ion batteries[J]. Carbon, 2022, 188: 238-245.

[144] Li G, Huang L B, Yan M Y, et al. An integral interface with dynamically stable evolution on micron-sized SiO_x particle anode[J]. Nano Energy, 2020, 74: 104890.

[145] Park S H, King P J, Tian R, et al. High areal capacity battery electrodes enabled by segregated nanotube networks[J]. Nature Energy, 2019, 4(7): 560-567.

[146] Zhang H, Zhang X, Jin H, et al. A robust hierarchical 3D Si/CNTs composite with void and carbon shell as Li-ion battery anodes[J]. Chemical Engineering Journal, 2019, 360: 974-981.

[147] Zhang Z, Han X, Li L, et al. Tailoring the interfaces of silicon/carbon nanotube for high rate lithium-ion battery anodes[J]. Journal of Power Sources, 2020, 450: 227593.

[148] Gao X, Wang F, Gollon S, et al. Micro silicon-graphene-carbon nanotube anode for full cell lithium-ion battery[J]. Journal of Electrochemical Energy Conversion and Storage, 2019, 16(1): 011009.

[149] Divakaran A M, Minakshi M, Bahri P A, et al. Rational design on materials for developing next generation lithium-ion secondary battery[J]. Progress in Solid State Chemistry, 2021, 62: 100298.

[150] Cheng H, Shapter J G, Li Y, et al. Recent progress of advanced anode materials of lithium-ion batteries[J]. Journal of Energy Chemistry, 2021, 57: 451-468.

[151] Liu Z, Yuan X, Zhang S, et al. Three-dimensional ordered porous electrode materials for electrochemical energy storage[J]. NPG Asia Materials, 2019, 11: 12.

[152] Issatayev N, Nuspeissova A, Kalimuldina G, et al. Three-dimensional foam-type current collectors for rechargeable batteries: A short review[J]. Journal of Power Sources Advances, 2021, 10: 100065.

[153] He Z, Wan T, Luo Y, et al. Three-dimensional structural confinement design of conductive metal oxide for efficient sulfur host in lithium-sulfur batteries[J]. Chemical Engineering Journal, 2022, 448: 137656.

[154] Cui G, Li G, Luo D, et al. Three-dimensionally ordered macro-microporous metal organic frameworks with strong sulfur immobilization and catalyzation for high-performance lithium-sulfur batteries[J]. Nano Energy, 2020, 72: 104685.

[155] Kim D-W, Zettsu N, Teshima K. Three-dimensional SWCNT and MWCNT hybrid networks for extremely high-loading and high rate cathode materials[J]. Journal of Materials Chemistry A, 2019, 7(29): 17412-17419.

[156] Liu Z, Wang J, Bi R, et al. Ultrasmall NiS_2 nanocrystals embedded in ordered macroporous graphenic carbon matrix for efficiently pseudocapacitive sodium storage[J]. Transactions of Tianjin University, 2023, 29(2): 89-100.

[157] Mageto T, Bhoyate S D, De Souza F M, et al. Developing practical solid-state rechargeable Li-ion batteries: Concepts, challenges, and improvement strategies[J]. Journal of Energy Storage, 2022, 55: 105688.

[158] Le T V, Nguyen H T, Luu A T, et al. $LiMn_2O_4$/CNTs and $LiNi_{0.5}Mn_{1.5}O_4$/CNTs nanocomposites as high-performance cathode materials for lithium-ion batteries[J]. ACTA Metallurgica Sinica-English Letters, 2015, 28(1): 122-128.

[159] Guo Y, Li X, Wang Z, et al. Free-standing ultrathick $LiMn_2O_4$@single-wall carbon nanotubes electrode with high areal capacity[J]. Journal of Energy Chemistry, 2022, 73: 452-459.

[160] Kumar J, Neiber R R, Park J, et al. Recent progress in sustainable recycling of $LiFePO_4$-type lithium-ion batteries: Strategies for highly selective lithium recovery[J]. Chemical Engineering Journal, 2022, 431: 133993.

[161] Roeder F, Ramasubramanian S. A review and perspective on path dependency in batteries[J]. Energy Technology, 2022, 10(11): 2200627.

[162] Cao H, Wen L, Guo Z Q, et al. Application and prospects for using carbon materials to modify lithium iron phosphate materials used at low temperatures[J]. New Carbon Materials, 2022, 37(1): 43-58.

[163] Gao C, Liu S, Yan P, et al. Enhanced electrochemical kinetics and three dimensional architecture lithium iron phosphate/carbon nanotubes nanocomposites for high rate lithium-ion batteries[J]. Colloids and Surfaces A: Physicochemical and Engineering Aspects, 2022, 643: 128718.

[164] Kang B, Ceder G. Battery materials for ultrafast charging and discharging[J]. Nature, 2009, 458(7235): 190-193.

[165] Wang B, Al Abdulla W, Wang D, et al. A three-dimensional porous $LiFePO_4$ cathode material modified with a nitrogen-doped graphene aerogel for high-power lithium ion batteries[J]. Energy & Environmental Science, 2015, 8(3): 869-875.

[166] Wang B, Liu T, Liu A, et al. A hierarchical porous C@$LiFePO_4$/carbon nanotubes microsphere composite for high-rate lithium-ion batteries: Combined experimental and theoretical study[J]. Advanced Energy Materials, 2016, 6(16): 1600426.

[167] Wang L, Liu T, Wu T, et al. Strain-retardant coherent perovskite phase stabilized Ni-rich cathode[J]. Nature, 2022, 611(7934): 61-67.

[168] Kim J H, Ahn J, Kim H M, et al. Highly efficient oxidation of single-walled carbon nanotubes in liquid crystalline phase and dispersion for applications in Li-ion batteries[J]. Chemical Engineering Journal, 2023, 458: 141350.

[169] Liu W, Zang Y, Qu J, et al. Dual functions of three-dimensional hierarchical architecture on improving the rate capability and cycle

performance of $LiNi_{0.8}Co_{0.1}Mn_{0.1}O_2$ cathode material for lithium-ion battery[J]. Ceramics International, 2022, 48(7): 9124-9133.

[170] Zhan Y X, Shi P, Ma X X, et al. Failure mechanism of lithiophilic sites in composite lithium metal anode under practical conditions[J]. Advanced Energy Materials, 2022, 12(2): 2103291.

[171] Chen J, Zhao J, Lei L, et al. Dynamic intelligent Cu current collectors for ultrastable lithium metal anodes[J]. Nano Letters, 2020, 20(5): 3403-3410.

[172] Huang J Q. Understanding interphases at the atomic scale[J]. Nature Nanotechnology, 2022, 17(7): 680-681.

[173] Huang Z, Lai J C, Liao S L, et al. A salt-philic, solvent-phobic interfacial coating design for lithium metal electrodes[J]. Nature Energy, 2023, 8(6): 577-585.

[174] Wang G, Chen C, Chen Y, et al. Self-stabilized and strongly adhesive supramolecular polymer protective layer enables ultrahigh-rate and large-capacity lithium-metal anode[J]. Angewandte Chemie-International Edition, 2020, 59(5): 2055-2060.

[175] Zhang J, Chen H, Wen M, et al. Lithiophilic 3D copper-based magnetic current collector for lithium-free anode to realize deep lithium deposition[J]. Advanced Functional Materials, 2022, 32(13): 2110110.

[176] Zhang C, Huang Z, Lv W, et al. Carbon enables the practical use of lithium metal in a battery[J]. Carbon, 2017, 123: 744-755.

[177] Zhu N, Yang Y, Li Y, et al. Carbon-based interface engineering and architecture design for high-performance lithium metal anodes[J]. Carbon Energy, 2023: e423.

[178] Xiang L, Zhang H, Hu Y, et al. Carbon nanotube-based flexible electronics[J]. Journal of Materials Chemistry C, 2018, 6(29): 7714-7727.

[179] Sun Z, Jin S, Jin H, et al. Robust expandable carbon nanotube scaffold for ultrahigh-capacity lithium-metal anodes[J]. Advanced Materials, 2018, 30(32): 1800884.

[180] Yang G, Li Y, Tong Y, et al. Lithium plating and stripping on carbon nanotube sponge[J]. Nano Letters, 2019, 19(1): 494-499.

[181] Yu G T, Chung S H. Rational design of a high-loading polysulfide cathode and a thin-lithium anode for developing lean-electrolyte lithium-sulfur full cells[J]. Small, 2023, 19(43): 2303490.

[182] Mei Y, Zhou J, Hao Y, et al. High-lithiophilicity host with micro/nanostructured active sites based on Wenzel wetting model for dendrite-free lithium metal anodes[J]. Advanced Functional Materials, 2021, 31(50): 2106676.

[183] Tan J, Soto F A, Noh J, et al. Large areal capacity and dendrite-free anodes with long lifetime enabled by distributed lithium plating with mossy manganese oxides[J]. Journal of Materials Chemistry A, 2021, 9(14): 9291-9300.

[184] Lu Q, Jie Y, Meng X, et al. Carbon materials for stable Li metal anodes: Challenges, solutions, and outlook[J]. Carbon Energy, 2021, 3(6): 957-975.

[185] Chadha U, Bhardwaj P, Padmanaban S, et al. Review-contemporary progresses in carbon-based electrode material in Li-S batteries[J]. Journal of the Electrochemical Society, 2022, 169(2): 020530.

[186] Seh Z W, Sun Y, Zhang Q, et al. Designing high-energy lithium-sulfur batteries[J]. Chemical Society Reviews, 2016, 45(20): 5605-5634.

[187] Chen Y T, Abbas S A, Kaisar N, et al. Mitigating metal dendrite formation in Lithium-Sulfur batteries via morphology-tunable graphene oxide interfaces[J]. ACS Applied Materials & Interfaces, 2019, 11(2): 2060-2070.

[188] Li X, Zhao X, Wang J, et al. A multifunctional separator based on dilithium tetraaminophthalocyanine self-assembled on rGO with improved cathode and anode performance in Li-S batteries[J]. Carbon, 2023, 201: 307-317.

[189] Yu L, Zhou X, Lu L, et al. MXene/carbon nanotube hybrids: Synthesis, structures, properties, and applications[J]. Chem Sus Chem, 2021, 14(23): 5079-5111.

[190] Chen L, Yu H, Li W, et al. Interlayer design based on carbon materials for lithium-sulfur batteries: a review[J]. Journal of Materials Chemistry A, 2020, 8(21): 10709-10735.

[191] Ali S, Rehman S a U, Luan H-Y, et al. Challenges and opportunities in functional carbon nanotubes for membrane-based water treatment and desalination[J]. Science of the Total Environment, 2019, 646: 1126-1139.

[192] Wang X, Hao X, Cai D, et al. An ultraviolet polymerized 3D gel polymer electrolyte based on multi-walled carbon nanotubes doped double polymer matrices for lithium-sulfur batteries[J]. Chemical Engineering Journal, 2020, 382: 122714.

[193] Yao W, Xu J, Ma L, et al. Recent progress for concurrent realization of shuttle-inhibition and dendrite-free lithium-sulfur batteries[J]. Advanced Materials, 2023, 35(32): 2212116.

[194] Li Z, Tang L, Liu X, et al. A polar TiO/MWCNT coating on a separator significantly suppress the shuttle effect in a lithium-sulfur battery[J]. Electrochimica Acta, 2019, 310: 1-12.

[195] Chung S H, Manthiram A. High-performance Li-S batteries with an ultra-lightweight MWCNT-coated separator[J]. Journal of Physical Chemistry Letters, 2014, 5(11): 1978-1983.

[196] Ponraj R, Kannan A G, Ahn J H, et al. Effective trapping of lithium polysulfides using a functionalized carbon nanotube-coated separator for lithium-sulfur cells with enhanced cycling stability[J]. ACS Applied Materials & Interfaces, 2017, 9(44): 38445-38454.

[197] Guan B, Zhang Y, Fan L, et al. Blocking polysulfide with Co_2B@CNT via “synergetic adsorptive effect” toward ultrahigh-rate capability and robust lithium-sulfur battery[J]. ACS Nano, 2019, 13(6): 6742-6750.

[198] Hong X J, Song C L, Yang Y, et al. Cerium based metal-organic frameworks as an efficient separator coating catalyzing the conversion of polysulfides for high performance lithium-sulfur batteries[J]. ACS Nano, 2019, 13(2): 1923-1931.

[199] Yao S, Cui J, Huang J Q, et al. Novel 2D Sb_2S_3 nanosheet/CNT coupling layer for exceptional polysulfide recycling performance[J]. Advanced Energy Materials, 2018, 8(24):

1800710.

[200] Pang Y, Wei J, Wang Y, et al. Synergetic protective effect of the ultralight MWCNTs/NCQDs modified separator for highly stable lithium-sulfur batteries[J]. Advanced Energy Materials, 2018, 8(10): 1702288.

[201] Lee Y H, Kim J H, Kim J H, et al. Spiderweb-mimicking anion-exchanging separators for Li-S batteries[J]. Advanced Functional Materials, 2018, 28(41): 1801422.

[202] Sun X, Huang Y, Chen M, et al. Double interlayers to improve cycle performance for Li-S batteries by using multiwall carbon nanotubes/reduced graphene oxide[J]. Industrial & Engineering Chemistry Research, 2018, 57(19): 6741-6745.

[203] Wang A, Xu G, Ding B, et al. Highly conductive and lightweight composite film as polysulfide reservoir for high-performance lithium-sulfur batteries[J]. ChemElectroChem, 2017, 4(2): 362-368.

[204] Sui D, Xu L, Zhang H, et al. A 3D cross-linked graphene-based honeycomb carbon composite with excellent confinement effect of organic cathode material for lithium-ion batteries[J]. Carbon, 2020, 157: 656-662.

[205] Huang J Q, Xu Z L, Abouali S, et al. Porous graphene oxide/carbon nanotube hybrid films as interlayer for lithium-sulfur batteries[J]. Carbon, 2016, 99: 624-632.

[206] Shi H, Zhao X, Wu Z S, et al. Free-standing integrated cathode derived from 3D graphene/carbon nanotube aerogels serving as binder-free sulfur host and interlayer for ultrahigh volumetric-energy-density lithium-sulfur batteries[J]. Nano Energy, 2019, 60: 743-751.

[207] Li H, Yang H, Ai X. Routes to electrochemically stable sulfur cathodes for practical Li-S batteries[J]. Advanced Materials, 2023: 2305038.

[208] Peng H J, Huang J Q, Cheng X B, et al. Review on high-loading and high-energy lithium-sulfur batteries[J]. Advanced Energy Materials, 2017, 7(24): 1700260.

[209] Zheng M, Chi Y, Hu Q, et al. Carbon nanotube-based materials for lithium-sulfur batteries[J]. Journal of Materials Chemistry A, 2019, 7(29): 17204-17241.

[210] Xiao Q, Yang J, Wang X, et al. Carbon-based flexible self-supporting cathode for lithium-sulfur batteries: Progress and perspective[J]. Carbon Energy, 2021, 3(2): 271-302.

[211] Chung S H, Chang C H, Manthiram A. Progress on the critical parameters for lithium-sulfur batteries to be practically viable[J]. Advanced Functional Materials, 2018, 28(28): 1801188.

[212] Helen M, Reddy M A, Diemant T, et al. Single step transformation of sulphur to Li_2S_2/Li_2S in Li-S batteries[J]. Scientific Reports, 2015, 5: 12146.

[213] Li Y, Li Z, Zhang Q, et al. Sulfur-infiltrated three-dimensional graphene-like material with hierarchical pores for highly stable lithium-sulfur batteries[J]. Journal of Materials Chemistry A, 2014, 2(13): 4528-4533.

[214] Zhou W, Yu Y, Chen H, et al. Yolk-shell structure of polyaniline-coated sulfur for lithium-sulfur batteries[J]. Journal of the American Chemical Society, 2013, 135(44): 16736-16743.

[215] Peng X X, Lu Y Q, Zhou L L, et al. Graphitized porous carbon materials with high sulfur loading for lithium-sulfur batteries[J]. Nano Energy, 2017, 32: 503-510.

[216] Li M, Carter R, Douglas A, et al. Sulfur vapor-infiltrated 3D carbon nanotube foam for binder-free high areal capacity lithium-sulfur battery composite cathodes[J]. ACS Nano, 2017, 11(5): 4877-4884.

[217] Kang W, Fan L, Deng N, et al. Sulfur-embedded porous carbon nanofiber composites for high stability lithium-sulfur batteries[J]. Chemical Engineering Journal, 2018, 333: 185-190.

[218] Pei F, Lin L, Ou D, et al. Self-supporting sulfur cathodes enabled by two-dimensional carbon yolk-shell nanosheets for high-energy-density lithium-sulfur batteries[J]. Nature Communications, 2017, 8: 482.

[219] Razzaq A A, Yao Y, Shah R, et al. High-performance lithium sulfur batteries enabled by a synergy between sulfur and carbon nanotubes[J]. Energy Storage Materials, 2019, 16: 194-202.

[220] Wang S, Feng S, Liang J, et al. Insight into MoS_2-MoN heterostructure to accelerate polysulfide conversion toward high-energy-density lithium-sulfur batteries[J]. Advanced Energy Materials, 2021, 11(11): 2003314.

[221] He J, Bhargav A, Manthiram A. In situ grown 1T'-$MoTe_2$ nanosheets on carbon nanotubes as an efficient electrocatalyst and lithium regulator for stable lithium-sulfur full cells[J]. Advanced Energy Materials, 2022, 12(1): 2103204.

[222] Guo B, Song G, Chen M, et al. FeCo alloy modified and carbon nanotube linked hollow carbon nanocages as efficient sulfur hosts for Li-S batteries[J]. Surfaces and Interfaces, 2023, 42.

[223] Manthiram Arumugam F Y. Advances in rechargeable lithium–sulfur batteries[M]. Springer, 2022.

[224] Fang R P, Li G X, Zhao S Y, et al. Single-wall carbon nanotube network enabled ultrahigh sulfur-content electrodes for high-performance lithium-sulfur batteries[J]. Nano Energy, 2017, 42: 205-214.

[225] Yuan Z, Peng H J, Huang J Q, et al. Hierarchical Free-Standing Carbon-Nanotube Paper Electrodes with Ultrahigh Sulfur-Loading for Lithium-Sulfur Batteries[J]. Advanced Functional Materials, 2014, 24(39): 6105-6112.

[226] Wu Q, Shadike Z, Xu J, et al. Integrated reactor architecture of conductive network and catalytic nodes to accelerate polysulfide conversion for durable and high-loading Li-S batteries[J]. Energy Storage Materials, 2023, 55: 73-83.

[227] Li H, Li Y, Zhang L. Designing principles of advanced sulfur cathodes toward practical lithium-sulfur batteries[J]. Sustainable Materials, 2022, 2(1): 34-64.

[228] Chen D, Zhang W, Luo K, et al. Hard carbon for sodium storage: mechanism and optimization strategies toward commercialization[J]. Energy & Environmental Science, 2021, 14(4): 2244-2262.

[229] Zhang T, Li C, Wang F, et al. Recent advances in carbon anodes for sodium-ion batteries[J]. Chemical Record, 2022, 22(10):

e202200083.

[230] Zheng Y, Zhang Z, Liu W, et al. Unveiling the Na-ions storage mechanism and sodiation-induced brittleness of multiwalled carbon nanotubes[J]. Journal of Power Sources, 2022, 532: 231357.

[231] Zhao Y, Hu Z, Fan C, et al. Constructing high-performance N-doped carbon nanotubes anode by tuning interlayer spacing and the compatibility mechanism with ether electrolyte for sodium-ion batteries[J]. Chemical Engineering Journal, 2022, 446: 137427.

[232] Aslam M K, Niu Y, Hussain T, et al. How to avoid dendrite formation in metal batteries: Innovative strategies for dendrite suppression[J]. Nano Energy, 2021, 86: 106142.

[233] Bai M, Tang X, Liu S, et al. An anodeless, mechanically flexible and energy/power dense sodium battery prototype[J]. Energy & Environmental Science, 2022, 15(11): 4686-4699.

[234] Qin M, Qin N, Lei M, et al. Construction of $Na_3V_2(PO_4)_2F_3$@C/CNTs nanocomposites with three-dimensional conductive network as cathode materials for sodium-ion batteries[J]. Journal of Electroanalytical Chemistry, 2022, 920: 116613.

[235] Yan Y, Ma Z, Lin H, et al. Hydrogel self-templated synthesis of $Na_3V_2(PO_4)_3$@C@CNT porous network as ultrastable cathode for sodium-ion batteries[J]. Composites Communications, 2019, 13: 97-102.

[236] Stoller M D, Park S, Zhu Y, et al. Graphene-based ultracapacitors[J]. Nano Letters, 2008, 8(10): 3498-3502.

[237] Pope M A, Korkut S, Punckt C, et al. Supercapacitor electrodes produced through evaporative consolidation of graphene oxide-water-ionic liquid gels[J]. Journal of the Electrochemical Society, 2013, 160(10): A1653-A1660.

[238] Miller J R, Simon P. Materials science-electrochemical capacitors for energy management[J]. Science, 2008, 321(5889): 651-652.

[239] Bo Z, Wen Z, Kim H, et al. One-step fabrication and capacitive behavior of electrochemical double layer capacitor electrodes using vertically-oriented graphene directly grown on metal[J]. Carbon, 2012, 50(12): 4379-4387.

[240] Cheng Q, Tang J, Ma J, et al. Graphene and carbon nanotube composite electrodes for supercapacitors with ultra-high energy density[J]. Physical Chemistry Chemical Physics, 2011, 13(39): 17615-17624.

[241] Cao C, Zhou Y, Ubnoske S, et al. Highly stretchable supercapacitors via crumpled vertically aligned carbon nanotube forests[J]. Advanced Energy Materials, 2019, 9(22): 1900618.

[242] Lu Z, Foroughi J, Wang C, et al. Superelastic hybrid CNT/Graphene fibers for wearable energy storage[J]. Advanced Energy Materials, 2018, 8(8): 1702047.

[243] Li X, Tang Y, Song J, et al. Self-supporting activated carbon/carbon nanotube/reduced graphene oxide flexible electrode for high performance supercapacitor[J]. Carbon, 2018, 129: 236-244.

[244] Kshetri T, Duy Thanh T, Dinh Chuong N, et al. Ternary graphene-carbon nanofibers-carbon nanotubes structure for hybrid supercapacitor[J]. Chemical Engineering Journal, 2020, 380: 122543.

[245] Pal M, Subhedar K M. CNT yarn based solid state linear supercapacitor with multi-featured capabilities for wearable and implantable devices[J]. Energy Storage Materials, 2023, 57: 136-170.

[246] Chen T, Dai L. Carbon nanomaterials for high-performance supercapacitors[J]. Materials Today, 2013, 16(7-8): 272-280.

[247] Kumar S, Nehra M, Kedia D, et al. Carbon nanotubes: A potential material for energy conversion and storage[J]. Progress in Energy and Combustion Science, 2018, 64: 219-253.

[248] Shearer C J, Cherevan A, Eder D. Application and future challenges of functional nanocarbon hybrids[J]. Advanced Materials, 2014, 26(15): 2295-2318.

[249] Hu L, Wu H, La Mantia F, et al. Thin, flexible secondary Li-ion paper batteries[J]. ACS Nano, 2010, 4(10): 5843-5848.

[250] 刘芯言, 彭翊杰, 黄佳琦, 等. 碳纳米管在柔性储能器件中的应用进展[J]. 储能科学与技术, 2013, 2(05): 433-450.
(Liu X Y, Peng H J, Huang J Q, et al. Carbon nanotubes for flexible energy storage devices-A review[J]. Energy Storage Science and Technology, 2013, 2(05): 433-450.)

[251] Das H T, Dutta S, Balaji T E, et al. Recent trends in carbon nanotube electrodes for flexible supercapacitors: A review of smart energy storage device assembly and performance[J]. Chemosensors, 2022, 10(6): 223.

[252] He J, Cao L, Cui J, et al. Flexible energy storage devices to power the future[J]. Advanced Materials, 2024, 36(4): 2306090.

[253] Zhu S, Zhang Z, Sheng J, et al. High-quality single-walled carbon nanotube films as current collectors for flexible supercapacitors[J]. Journal of Materials Chemistry A, 2023, 11(24): 12941-12949.

[254] Lu P, Jiang X, Guo W, et al. A Ni-Co sulfide nanosheet/carbon nanotube hybrid film for highenergy and high-power flexible supercapacitors[J]. Carbon, 2021, 178: 355-362.

[255] Zhu S, Sheng J, Chen Y, et al. Carbon nanotubes for flexible batteries: recent progress and future perspective[J]. National Science Review, 2021, 8(5): 261.

[256] Jo S, Lee K, Jung Y, et al. Direct-spun carbon nanotube sheet: A flexible, ultralight, stackable three-dimensional current collector for high-performance lithium-ion batteries[J]. Carbon, 2024, 219: 118786.

[257] Hong Z X, Fang Z H, Luo Y F, et al. Promising nano-silicon anodes prepared using the “disperse-anchor” strategy and functional carbon nanotube interlayers for flexible lithium-ion batteries[J]. Journal of Materials Chemistry A, 2022, 10(44): 23509-23520.

[258] Chen L, Yuan Y, Orenstein R, et al. Carbon materials dedicate to bendable supports for flexible lithium-sulfur batteries[J]. Energy Storage Materials, 2023, 60: 102817.

[259] Luo J, Liu X, Lei W, et al. Self-standing lotus root-like host materials for high-performance lithium-sulfur batteries[J]. Advanced Fiber Materials, 2022, 4(6): 1656-1668.

[260] Jo S C, Hong J W, Choi I H, et al. Multimodal capturing of polysulfides by phosphorus-doped carbon composites for flexible high-energy-density lithium-sulfur batteries[J]. Small, 2022, 18(21): 2200326.

[261] Liu F, Feng P, Yuan M, et al. Continuous preparation of a flexible carbon nanotube film from lignin as a sulfur host material for lithium-sulfur batteries[J]. ACS Sustainable Chemistry & Engineering, 2023, 11(46): 16544-16553.

[262] Wei M, Zhu H, Zhai P, et al. Nano-sulfur confined in a 3D carbon nanotube/graphene network as a free-standing cathode for high-performance Li-S batteries[J]. Nanoscale Advances, 2022, 4(22): 4809-4818.

[263] Yang F, Zhao H F, Li R M, et al. Growth modes of single-walled carbon nanotubes on catalysts[J]. Science Advances, 2022, 8(41): eabq0794.

[264] Liu X Y, Li Z H, Chong B Y, et al. Electrochemically dealloying engineering toward integrated monolithic electrodes with superior electrochemical Li-storage properties[J]. Small, 2024, 20(40): 2401698.

[265] Zhang F, Hou P X, Liu C, et al. Growth of semiconducting single-wall carbon nanotubes with a narrow band-gap distribution[J]. Nature Communications, 2016, 7: 11160.

[266] Zhang Y, Li Y, Wen H, et al. Length-controlled sorting and length-dependent properties of short semiconducting single-walled carbon nanotubes[J]. Carbon, 2023, 215: 118468.

[267] Gu J, Han J, Liu D, et al. Solution-processable high-purity semiconducting SWCNTs for large-area fabrication of high-performance thin-film transistors[J]. Small, 2016, 12(36): 4993-4999.

[268] Song B, Yang J, Zhao J, et al. Intercalation and diffusion of lithium ions in a carbon nanotube bundle by ab initio molecular dynamics simulations[J]. Energy & Environmental Science, 2011, 4(4): 1379-1384.

[269] Shi Q Q, Zhan H, Zhang Y, et al. Highly flexible and free-standing carbon nanotube/hollow carbon nanocage hybrid films for high-performance supercapacitors[J]. RSC Advances, 2021, 11(12): 6655-6661.

[270] Kim M, Goerzen D, Jena P V, et al. Human and environmental safety of carbon nanotubes across their life cycle[J]. Nature Reviews Materials, 2024, 9(1): 63-81.